

# On the Informativeness of Supervision Signals

Ilia Sucholutsky<sup>1</sup>   Ruairidh M. Battleday<sup>1</sup>   Katherine M. Collins<sup>2</sup>   Raja Marjeh<sup>3</sup>   Joshua C. Peterson<sup>1</sup>  
 Pulkit Singh<sup>1</sup>   Umang Bhatt<sup>2,4</sup>   Nori Jacoby<sup>5</sup>   Adrian Weller<sup>2,4</sup>   Thomas L. Griffiths<sup>1,2</sup>

<sup>1</sup>Dept. of Computer Science, Princeton University,

<sup>2</sup>Dept. of Engineering, University of Cambridge,

<sup>3</sup>Dept. of Psychology, Princeton University,

<sup>4</sup>Alan Turing Institute,

<sup>5</sup>Max Planck Institute for Empirical Aesthetics

## Abstract

Supervised learning typically focuses on learning transferable representations from training examples annotated by humans. While rich annotations (like soft labels) carry more information than sparse annotations (like hard labels), they are also more expensive to collect. For example, while hard labels only provide information about the closest class an object belongs to (e.g., “this is a dog”), soft labels provide information about the object’s relationship with multiple classes (e.g., “this is most likely a dog, but it could also be a wolf or a coyote”). We use information theory to compare how a number of commonly-used supervision signals contribute to representation-learning performance, as well as how their capacity is affected by factors such as the number of labels, classes, dimensions, and noise. Our framework provides theoretical justification for using hard labels in the big-data regime, but richer supervision signals for few-shot learning and out-of-distribution generalization. We validate these results empirically in a series of experiments with over 1 million crowdsourced image annotations and conduct a cost-benefit analysis to establish a tradeoff curve that enables users to optimize the cost of supervising representation learning on their own datasets.

## 1 INTRODUCTION

Modern machine learning relies heavily on using large amounts of labeled data, and those labels typically come from annotations generated by humans. This raises an important question: how can we most efficiently use human annotations to create objective functions for machine learning systems? This is not just a matter of designing good interfaces and algorithms for collecting annotations—it in-

volves a subtle interplay between the choices we make about the supervision signals we use to train our models and the difficulty of collecting the relevant annotations. For example, soft labels for images (indicating uncertainty via a distribution over classes) are more expensive to collect than hard labels (indicating a single class), but are also potentially more informative to the learner [Peterson et al., 2019, Sucholutsky and Schonlau, 2021b,a, Collins et al., 2022]. Making good choices about what questions to ask humans about our data requires understanding the informativeness of different supervision signals.

In this paper, we explore this question for the case of *representation learning*, where the aim is to learn useful latent embeddings of input stimuli. Generally, training a neural network means learning successive layers of representations that will be used to perform some sort of task (e.g., classification). The key decision in implementing a representation-learning framework often revolves around designing a supervision signal by quantifying the similarity between stimuli. Significant work has gone into the design of supervision signals for deep representation learning resulting in contrastive objectives [Chen et al., 2020, Khosla et al., 2020], classification objectives [Huh et al., 2016, Ridnik et al., 2021], reconstruction objectives [Devlin et al., 2018, Kingma and Welling, 2013], and many others [Guo et al., 2019]. For example, recent work has shown that models trained with hard labels on classification tasks can approximate the structure of human latent representations at a fraction of the cost of exhaustively collecting the pairwise-similarity judgments required for soft contrastive learning [Peterson et al., 2018, Marjeh et al., 2022]. Thus, in many cases, multiple representation learning objectives could work, and it is not clear when one objective should be preferred.

Our goal in this paper is to compare the informativeness of various supervision signals (i.e. types of annotations) to **empower researchers to optimize data annotation for their supervised representation learning tasks** (see Figure 1). We **develop an information-theoretic framework (Section 3)** for analyzing supervision signals and use it to

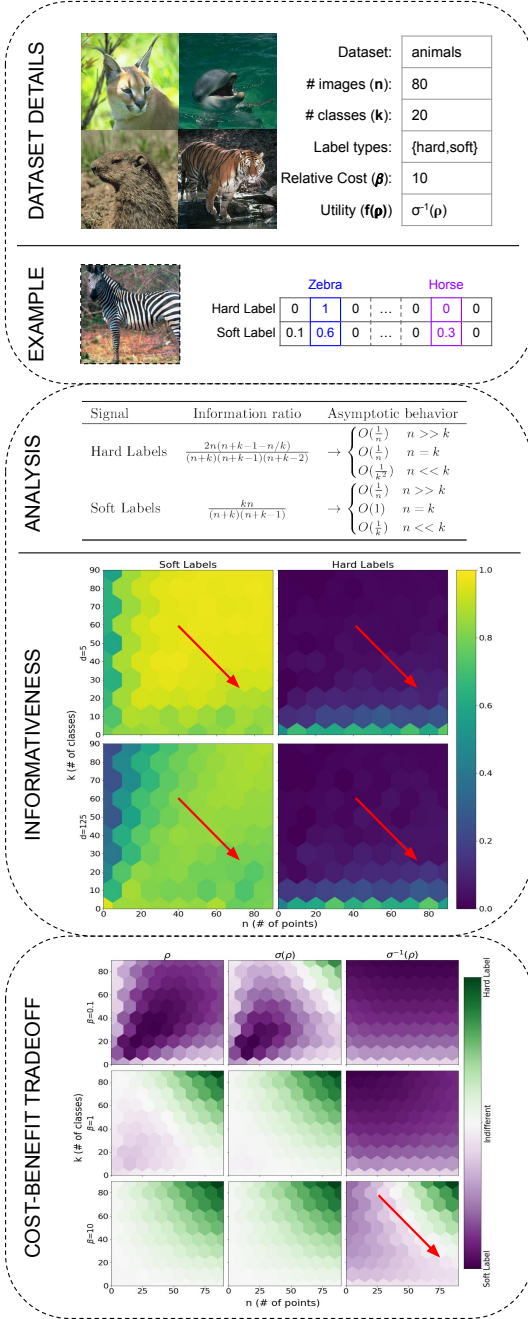


Figure 1: An example workflow for using our framework to decide what label type(s) to collect when annotating a dataset. **Top:** User specifies the task. **Middle:** Information-theoretic characterization of the task (e.g., many classes, but few examples). Heatmaps show correlation ( $\rho$ ) of ground-truth similarities with pairwise similarities recovered from simulated labels when varying latent dimensionality ( $d$ ), number of points ( $n$ ), and number of classes ( $k$ ). **Bottom:** Cost-benefit analysis of signal type based on subjective utility ( $u(\rho)$ ), cost ( $\beta$ ), number of points ( $n$ ), and number of classes ( $k$ ). Red arrows point to cells corresponding to the user-specified dataset.

compare two popular supervision signals from the classification literature—hard labels and soft labels. We quantify their relative (representational) information content by comparing them to similarity triplets (i.e., queries of the form “Is  $x$  more similar to  $y$  than to  $z$ ?”), a supervision signal used in contrastive learning and cognitive science [Jamieson and Nowak, 2011, Hoffer and Ailon, 2015]. We relate the information each signal provides to three common features of machine learning datasets: number of labels, number of classes, and dimensionality, and find that while both hard and soft labels provide information about hidden representations, their responses to these three variables are very different. **Simulations confirm these results (Section 4)**, showing how the marginal information provided by each label translates into better representation learning performance. **A cost-benefit analysis (Section 5)** comparing soft and hard labels shows there are meaningful differences between them: soft labels are expensive to collect but provide a considerable amount of representational information while hard labels are cheap but fairly uninformative (Figure 1). To close this gap, we consider several types of sparse representations that enable selective interpolation between the soft- and hard-label regimes (Figures 2, 3). We extend our analysis with these sparse supervision signals to **establish a tradeoff curve allowing users to optimize the cost of labeling their datasets for supervised representation learning (Section 6)**. Finally, we confirm the theoretical and simulation results by **human experiments (Section 7)** with crowdsourced similarity judgments and various types of soft and hard labels collected for CIFAR-10 [Krizhevsky et al., 2009].

## 2 BACKGROUND

Throughout this paper, we discuss a variety of supervision signals. In this section, we identify the practical settings these signals correspond to and summarize related work.

**Pairwise similarity judgments:** For every pair of points in the dataset labelers are asked to rate the similarity on a fixed, bounded scale (e.g., a Likert scale). This signal has a long history of being employed by cognitive scientists to learn about (hidden) human representations of stimuli, typically by using an embedding method like multi-dimensional scaling (MDS) [Shepard, 1980], and more recently can be found in state-of-the-art contrastive learning objectives [Chen et al., 2020, Khosla et al., 2020].

**Triplet similarity judgments:** For every set of three points  $x, y, z$  in the dataset, labelers are asked to respond to queries of the form “Is  $x$  closer to  $y$  than to  $z$ ?” This non-metric signal has also been used as a method for learning human representations, often by applying embedding techniques like non-metric MDS [Jamieson and Nowak, 2011, Agarwal et al., 2007, Davenport, 2013]; it is considered to be a more accurate alternative to pairwise similarity judgments as it

is easier to compare two lengths than to provide consistent judgments over un-normalized scales. This signal is used in machine learning (typically with the triplet loss) and cognitive science [Hoffer and Ailon, 2015, Hermans et al., 2017, Hebart et al., 2020, Roads and Love, 2021].

**Hard labels:** For each point, labelers pick a single, most relevant class out of the fixed set of all classes in the dataset. This signal is typically used for classification, though it can also be used for representation learning via pre-training [Huh et al., 2016, Ridnik et al., 2021].

**Soft labels:** For each point, labelers assign proximity or probability to each of the fixed set of all classes in the dataset. This signal is also used for classification and representation learning via pre-training, and can be more effective than hard labels, particularly in settings with small data [Xie et al., 2020, Sucholutsky and Schonlau, 2021a, Sucholutsky et al., 2021, Liu et al., 2021, Malaviya et al., 2022].

**Top-class soft labels:** The researcher picks a subset of size  $\hat{k}$  of the classes in the dataset that maximize mutual information (estimated based on the already collected subset). For each point, labelers assign proximity or probability to each of the fixed set of classes in the subset. The number of classes can be reduced by simply taking an arbitrary subset, or more systematically via methods like label coarsening [Hanneman and Lavie, 2011].

**Sparse soft labels:** For each point, labelers assign proximity or probability to each of the exactly  $\hat{k}$  most relevant classes out of the fixed set of all classes in the dataset [Collins et al., 2022]. In addition to the connections discussed above for the other soft label variants, this particular variant is also connected to top-k classification [Lapin et al., 2017] and soft vector quantization [Seo and Obermayer, 2003].

### 3 RELATIVE INFORMATIVENESS OF SUPERVISION SIGNALS

**Setup:** We consider the scenario where a researcher collects an initial set of labels for a small subset of their dataset and wants to use it to optimize the labelling of their entire dataset (Figure 1, top). The researcher has a number of options for what kind of labels to collect and wishes to maximize representation learning performance while minimizing labelling cost. We formalize representation learning as the process of recovering a hidden (low-dimensional) latent structure from a set of (high-dimensional) stimuli (e.g. images). In particular, we focus on the non-metric setting where we want to recover the correct rank order of pairwise distances between all latent vectors. Our goal is to determine which supervision signal is most effective (in terms of both performance and cost) for representation learning.

**Problem Definition:** Consider a set of stimuli  $\{x_i\}_{i=1}^n \in \mathbb{R}^d$  with some associated latent representations  $\{z_i\}_{i=1}^n \in$

$\mathbb{R}^h$ . The distance between each pair of latent vectors induces a relational order over latent pairs and our goal is to find a function  $f : \mathbb{R}^d \rightarrow \mathbb{R}^h$  (where typically  $h \ll d$ ) such that it preserves this relational order, that is,  $\|f(x_i) - f(x_j)\| \leq \|f(x_i) - f(x_k)\|$  iff  $\|z_i - z_j\| \leq \|z_i - z_k\|$ . Crucially, the latent vectors are accessible only implicitly via different supervision signals (or queries) such as hard and soft labels. We operationalize the informativeness of different supervision signals as the number of relational constraints that a naive learner can recover based on them (i.e., a learner that attempts to follow the signals as is without applying other geometric constraints such as triangle inequalities).

**Triplet Constraints:** Conceptually, when training a neural network for classification, providing a label for a point roughly corresponds to requiring that the network weights should be updated such that the embedding of this point will be closer to one class than to other classes. For this analysis, we assume that each class can be represented by its centroid (e.g., each class is unimodal), and so classification labels provide information about proximity of latent vectors to these centroids<sup>1</sup>. When training with batches, providing labels for a batch additionally corresponds to requiring that the centroid of each class be closer to its associated set of embeddings than to the other embeddings in the batch. In both cases, neural networks are optimizing constraints of the form “ $x$  is closer to  $y$  than to  $z$ ,” which we call “triplet constraints”. We now formalize this concept to use it as a measure of information content in labels.

Suppose we have a system with  $n$  labels,  $k$  classes with centroids  $C_1, \dots, C_k$ , and stimuli  $\{x_i\}_{i=1}^n$  with latent representations  $\{z_i\}_{i=1}^n$ . A triplet constraint is an inequality of the form  $\|z_a - z_b\| < \|z_a - z_c\|$ . This can be rewritten as the query  $r_{i,j,k} = \{x \in \mathbb{R}^d : \|f(x_j) - f(x_i)\| < \|f(x_k) - f(x_i)\|\}$ , and each such query provides at most one bit of information as it cuts in half the space where  $x_i$  can be located [Jamieson and Nowak, 2011]. For any set of three stimuli, there are three unique queries:  $r_{i,j,k}, r_{j,i,k}, r_{k,i,j}$ . Thus, the total number of unique queries for  $n$  stimuli is  $3\binom{n}{3}$ . However, in the case of hard and soft labels, we make queries not only in terms of the  $n$  objects but also in terms of the  $k$  class centroids. In other words, we are seeking to recover embeddings not only for the  $n$  points of interest, but also  $k$  additional reference embeddings. As a result, the total number of unique queries in these cases is  $3\binom{n+k}{3}$ .

**Hard Labels:** We define the hard label for stimulus  $x$  as a vector  $l$  of length  $k$ , such that  $l_i = 1$  if  $i = \arg \min_j (\|f(x) - f(C_j)\|)$  and 0 otherwise. We can now extract two types of triplet queries. The first is a triplet consisting of a class centroid  $C_i$ , a stimulus  $x_P$  that is a “positive” example of this class, and a negative example

<sup>1</sup>This can easily be generalized to multi-modal classes by treating them as compositions of multiple unimodal subclasses (i.e. for an  $m$ -modal class,  $m$  centroids need to be learned).

stimulus  $x_N$ . The query has the form  $\|f(x_P) - f(C_i)\| < \|f(x_N) - f(C_i)\|$ . The second is a triplet consisting of a stimulus  $x_i$ , the class centroid that is closest to it ( $C_P$ ), and another class centroid further away ( $C_N$ ). This query has the form  $\|f(C_P) - f(x_i)\| < \|f(C_N) - f(x_i)\|$ . If the hard labels are distributed evenly between  $k$  classes, then on average there are  $n/k$  stimuli per class. Then  $n$  hard labels give us  $n(k-1)$  constraints of the second type and  $k(n/k)(n - n/k) = n^2(1 - 1/k)$  of the first type—a total of  $T_H(n, k) = n(k-1) + n^2(1 - 1/k)$  constraints.

**Soft Labels:** To produce a probability distribution over classes, neural networks often have a softmax activation function after the output layer [Bridle, 1989, Martins and Astudillo, 2016, Krizhevsky et al., 2017]. Accordingly, we define the soft label for a stimulus  $x$  as a vector  $l$  of length  $k$ , such that  $l_i = \frac{e^{-\|f(x) - f(C_i)\|}}{\sum_j e^{-\|f(x) - f(C_j)\|}}$ . There are again two types of triplet queries that we can extract from soft labels. The first is a triplet of the form  $\|f(x_P) - f(C_i)\| < \|f(x_N) - f(C_i)\|$  where  $C_i$  is the centroid of class  $i$  and  $x_P, x_N$  are two training set points with corresponding soft labels  $l^P, l^N$  such that  $l_i^P > l_i^N$ . The second is a triplet consisting of the form  $\|f(x) - f(C_i)\| < \|f(x) - f(C_j)\|$  where  $x$  is a training set point corresponding to label  $l$  and  $C_i, C_j$  are the centroids of classes  $i, j$  such that  $l_i > l_j$ . Our  $n$  soft labels thus give us  $nk(k-1)/2$  constraints of the second type and  $kn(n-1)/2$  of the first—a total of  $T_S(n, k) = kn(k+n-2)/2$  triplet constraints.

**Information Ratio:** While we now have a measure of how much information each label provides, it is unclear how much information is actually needed to recover human-aligned representations for all the objects. Intuitively, we would expect that more information is required when more objects are being embedded (i.e. when  $n+k$  increases). We can normalize our results from the previous section to account for this by taking the ratio of the number of constraints we can recover from a set of labels to the total number of possible queries (i.e.  $IR(n, k) = \frac{T(n, k)}{3^{\binom{n+k}{3}}}$ ). This “information ratio” may be a proxy for how much information we are recovering about the latent representations. We present the information ratios for hard and soft labels in the “Analysis” portion of Figure 1 along with their asymptotic behavior in three regimes: the many-shot case (where there are many more points than classes), the one-shot case (where there is one point per class; [Fei-Fei et al., 2006]), and the less-than-one-shot case (where there are fewer points than classes; [Sucholutsky and Schonlau, 2021a]).

Our results predict three scaling phases for soft labels and two scaling phases for hard labels. In particular, hard labels and soft labels are predicted to have similar asymptotic behavior in the many-shot case which may explain why pre-training on very large datasets using hard-label classification is effective (e.g. [Huh et al., 2016, Ridnik et al., 2021]). However, soft labels are predicted to have much bet-

ter representation learning performance in the one-shot and less-than-one-shot cases. Notably, the results predict that in the one-shot case, the quality of representations learned from soft labels should not degrade (as it does in every other case) when the number of points and classes increases.

**Representation Learning as Communication:** Our representation learning setup can be seen as a communication problem where we want to recover a fixed number of bits about hidden representations of a black-box model. The model can be queried via multiple channels, each of which has its own encoder and corresponds to a different choice of supervision signal. As established by Jamieson and Nowak [2011], each triplet query is a single bit. In information theory, the efficiency, also known as the normalized entropy, of each channel is defined as  $\eta(X) = \frac{H(X)}{H_{max}(X)}$  where  $H_{max}$  is max entropy (i.e. the total number of bits) and  $H$  is entropy (i.e. the number of bits remaining with unknown states after transmission). We defined information ratio as the ratio of the number of bits recovered to the total number of bits, and thus a stochastic version of information ratio (with data sampled from a distribution instead of being fixed) can be defined as  $IR(X) = \frac{H_{max}(X) - H(X)}{H_{max}(X)} = 1 - \eta(X)$ .

**Signal-to-Noise Ratio:** Our triplet analysis implicitly assumed that the noise distribution was the same between each type of label and could thus be ignored when comparing their relative informativeness. However, in practice, eliciting different kinds of annotations may be associated with different levels of noise due to changes in difficulty, user interface, participant pools, etc. Within our information-theoretic framework, noise can be viewed as the probability  $\epsilon_s$  of a bit flip (i.e. that we get the incorrect response to a query of the form “Is  $x$  closer to  $y$  than to  $z$ ?”) during communication over channel  $s$ . If a set of  $n$  labels (with  $k$  classes) of type  $s$  provides  $T_s(n, k)$  triplet constraints under our framework in the noise-free case, then the number of constraints in the noisy case is just  $(1 - \epsilon_s)T_s(n, k)$  where  $\epsilon_s$  is the bit flip rate for labels of type  $s$ .

## 4 SIMULATIONS

Our analysis predicts soft labels should generally lead to better performance than hard labels, particularly when there are few labels and many classes. However, we still need to understand how information ratios actually translate to representation learning performance. We conducted simulations to see the effect of four variables (and their interactions) on performance: label type (soft or hard), number of points ( $n$ ), number of classes ( $k$ ), and latent dimension ( $d$ ). We consider values of  $n$  and  $k$  in the range of  $[3, 90]$ , and  $d \in \{5, 25, 125\}$ . For each combination of  $n, k, d$  we sample a total of  $n$  points from Gaussians centered at  $k$  random locations  $C_1, \dots, C_k \in \mathbb{R}^d$ . We computed hard and soft labels for these points using the equations defined above

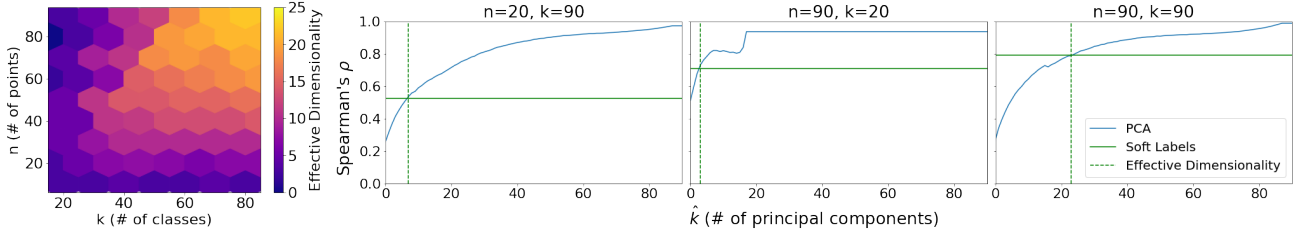


Figure 2: **Left:** Effective dimensionality of soft labels at different combinations of  $n$  and  $k$ . **Right:** Three examples of PCA curves used to compute effective dimensionality of soft labels for every combination of  $n$  and  $k$ .

and then mine all triplet constraints of both types from both sets of labels. We apply Generalized Nonmetric Multi-Dimensional Scaling (GNMDS; Davenport [2013]) to both sets of queries to find embeddings that best fit the respective triplet constraints. The Gram matrix outputted by GNMDS can be interpreted as predicted (unnormalized) pairwise cosine similarities between all  $n + k$  points and centroids.

To understand how much information we recover from each of these two sets of queries, we construct a matrix of the true pairwise cosine similarities for the set of all  $n + k$  points and class centroids and compute the Spearman rank correlation ( $\rho$ ) between the upper triangle of the Gram matrices and the ground truth matrix. Thus, a higher  $\rho$  corresponds to better recovery of the underlying latent representations. We visualize the simulation results in Figure 1. The results confirm the theoretical findings from the previous section. Specifically, the three phases for soft labels and two phases for hard labels match our analytical results, and **a higher information ratio translates into better performance**.

## 5 COST-BENEFIT TRADEOFFS

We can now construct cost-benefit tradeoff curves to **determine when a user would prefer to use one signal over the other**. Suppose we define  $\rho$  as above, and subjective utility as  $U(\rho)$ . This utility function can take many forms (e.g.,  $U(\rho) = b\rho$  or  $b\sigma(\rho)$  where  $\sigma$  is the sigmoid function and  $b > 0$ ). If we assume that the cost of collecting a soft label over  $k$  classes is about  $k$  times more expensive than collecting a hard label, we can define the subjective loss function as  $L_s = C(s) - U(\rho)$ , where  $C(s) = cn$  if  $s \in S_{hard}$  and  $cnk$  if  $s \in S_{soft}$ . This is equivalent to optimizing  $\hat{L} = \frac{c}{b}\hat{c}(s) - \hat{u}(\rho)$  which we can re-parametrize to a form reminiscent of the information bottleneck [Tishby et al., 2000]:  $\hat{L} = \beta\hat{c}(s) - \hat{u}(\rho)$ . Since we have shown that the information ratio, which we define as  $\hat{\rho}$ , can provide us with an estimate for  $\rho$ , we can also replace  $U(\rho)$  by  $U(\hat{\rho})$ .

We investigate cost-benefit tradeoffs by varying  $(\beta, \hat{u})$ , showing the results for several combinations in Figure 1. While the results depend greatly on choice of  $\hat{u}$ , a few regularities emerge. First, in all cases, regardless of  $\beta$ , when the number of classes ( $k$ ) or the number of points ( $n$ ) is low,

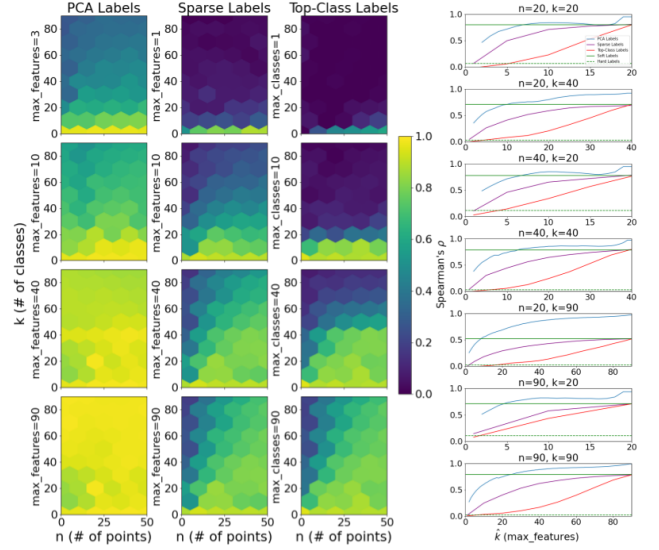


Figure 3: Label sparsity. **Left:** Spearman rank correlation ( $\rho$ ) of pairwise similarities recovered from PCA labels, sparse labels, and top-class labels when varying the maximum number of features/classes in the labels ( $\hat{k}$ ), number of points in the dataset ( $n$ ), and number of classes in the dataset ( $k$ ). **Right:** Comparison of sparsity curves for PCA labels (blue), sparse labels (purple), and top-class labels (red) for several combinations of  $n$  and  $k$ . Straight lines correspond to soft label (solid green) and hard label (dashed green) performance.

soft labels are roughly as preferred as, or more preferred, than hard labels. Second, when there is an emphasis on cost (i.e. high  $\beta$ ), hard labels become preferable as  $n$  and  $k$  both increase, but when the emphasis is on performance (i.e. low  $\beta$ ), soft labels remain preferable as  $n$  and  $k$  increase.

## 6 LABEL OPTIMIZATION

**Effective Dimensionality:** While soft labels appear to be more informative than hard labels, they are not necessarily an optimal encoding for efficiently communicating information about representations. In order to study how an optimal encoding might perform, we run principal component analysis (PCA) on our simulated datasets and observe the effects of varying the number of PCs that are retained ( $\hat{k}$ ). The resulting performance curves provide an approximate upper

bound on how well any set of vectors of length  $\hat{k}$  (e.g. a set of soft labels) can communicate information about representations. We can also use these curves to understand how efficient soft labels are at this task. Specifically, we define the “effective dimensionality” of a set of soft labels as the minimum number of PCs ( $\hat{k}$ ) necessary to achieve the same representation learning performance as when using the soft labels in the way we described in the previous section. In Figure 2, we show the effective dimensionality of soft labels for different combinations of  $n$  and  $k$  along with several examples of the PCA curves. We found a strong positive correlation between information ratio and effective dimensionality ( $r = 0.734, p < 10^{-15}$ ) providing further evidence information ratio is a useful metric for evaluating representation learning signals and predicting performance.

**Label Sparsity:** Since the effective dimensionality of soft labels appears to generally be much lower than the number of components of each soft label ( $k$ ), this suggests that soft labels are an inefficient encoding for representational information, potentially due to redundancy. We now investigate two methods for remedying this inefficiency by introducing sparsity into soft labels in a disciplined manner.

The first method, which we call “top-class soft labels”, introduces sparsity globally by ignoring classes that are the least informative across the entire dataset. Formally, we construct a matrix  $X$  where the  $i$ -th row correspond to the  $i$ -th soft label and the  $j$ -th column corresponds to the  $j$ -th class, and estimate the mutual information between each column and the ground-truth similarity matrix. We then keep only the top  $k$  most informative columns and set the rest to 0.

The second method, which we call “sparse soft labels”, is to introduce sparsity locally by ignoring classes that are least informative for each point. Formally, we again construct a matrix  $X$  as above, but now for each row, we individually keep only the  $\hat{k}$  largest components and set the rest to 0. These two methods provide a way to reduce the cost of collecting soft labels, while retaining much of the information.

In Figure 3, we visualize representation learning performance when using PCA, sparse labels, or top-class labels at different levels of sparsity. While sparse labels consistently outperform top-class labels (which is to be expected since sparse labels provide finer control over how sparsity is induced), we note that there is also a gap between PCA and sparse labels. This again suggests that it may be possible to design more effective labeling methods than soft labels, potentially by defining a search space over possible classes and applying a procedure like PCA to optimize over it. We leave this as a promising direction for future work.

**Optimizing Label Collection:** Since top-class and sparse labels provide a way to selectively interpolate between the soft label and hard label regime, we can now use sparsity to optimize the cost-benefit tradeoff curves discussed above beyond the binary preference optimization shown at the bot-

tom of Figure 1. We use the same loss functions as above with several combinations of cost parameter  $\beta$  and utility function  $\mu$ , but we now apply them to top-class and sparse labels at various levels of sparsity ( $\hat{k}$ ). We visualize a number of these cost-benefit tradeoff curves in the Supplement. By picking the  $\hat{k}$  that corresponds to minimal loss, we can now optimize our label collection to minimize cost while maximizing performance. The results suggest that **using sparse labels and picking the right level of sparsity ( $\hat{k}$ ) can often provide big gains** as opposed to using either hard labels or regular (dense) soft labels.

## 7 EXPERIMENTS

In this section, we investigate how our theory applies to real soft labels crowdsourced from human annotators. First, we present several methods for collecting soft labels—including new sets of annotations that we crowdsource for this study—and place them into the framework described above. Second, we use a large dataset of similarity judgements to assess the informativeness of the different label types. Finally, we assess how the inductive biases conferred by different label types affect the classification performance of a range of convolutional neural networks (CNNs).

### 7.1 EXPERIMENTAL SETUP

We consider a range of supervision signals over the *testing* subset of CIFAR-10 images [Krizhevsky et al., 2009], including hard labels, smoothed hard labels, soft labels, and similarity judgments. Each label type represents a different supervision signal presented in Section 2. Each type of soft label was collected using different experimental interfaces, details of which are in the Supplement.

**CIFAR-10H:** The CIFAR-10H labels, originally collected by Peterson et al. [2019], Battleday et al. [2020], are derived by averaging over 500,000 crowdsourced hard labels (roughly 50 per image). These are then normalized at the image level to return probability distributions.

**CIFAR-10DS:** The CIFAR-10DS labels, made up of over 500,000 judgments we crowdsourced for this study, are *dense* soft labels (i.e., assigned over all classes in CIFAR-10). Annotators provided numerical judgments on a 0 (not at all) to 1 (completely) scale using sliders depending on how well each category described a certain image.

**CIFAR-10S:** The CIFAR-10S labels from Collins et al. are *sparse soft labels*. Annotators provided around 20,000 judgments about the likelihood of the top two categories for each image and any categories which they believed were definitely wrong (referred to as a “clamp”, and assigned zero probability). As the authors only collected such labels over 1,000 examples from the test set, we in-fill the remaining 9,000 with either: 1) hard labels (CIFAR-10S+hard) or



2) simulated top-2 soft labels (CIFAR-10S+dense).

**CIFAR-10T** The CIFAR-10T labels are a novel set of labels we crowdsourced, comprising over 350,000 typicality ratings for each image under the ground truth category (about 35 judgements per image). 1759 unique participants were recruited on Amazon Mechanical Turk, and presented with a sequence of 200 randomly sampled CIFAR-10 test set images, upsampled to 160x160 pixels (see Peterson et al. [2019], Battleday et al. [2020]). Participants were given the category of each image, and asked to rate how typical it was of the category on a sliding scale of “Not at all typical” to “Extremely typical”. We interpret an image’s typicality as the probability of the ground truth class, and spread the remaining probability mass over the 9 remaining labels—a smoothed version of a *sparse* soft label with  $K=1$ ).

**CIFAR-10LS:** We derive two more sets of soft labels by applying label smoothing (LS) to the CIFAR-10 hard labels. Unlike human-derived soft labels, the “softness” here is applied uniformly and independently of the associated image. This allows us to control for the previously observed regularization effects of label smoothing [Müller et al., 2019]. We pick the smoothing rate,  $\epsilon$ , to roughly match the distributions of our crowdsourced labels. The “low” level,  $\epsilon \approx 0.05$ , is the average probability mass per soft label for the 9 non-maximal categories in the CIFAR-10H dataset. The “high” level,  $\epsilon \approx 0.2$ , matches the CIFAR-10DS dataset.

**Similarity Judgments:** We elicited a total of 49,500 pairwise similarity judgments over two subsets each consisting of 100 CIFAR-10 test set images by having human annotators rate the similarity between unlabeled image pairs on a Likert-scale ranging from 0 (completely dissimilar) to 6 (completely similar). The images were deliberately chosen to be ambiguous about class (see Supplement).

## 7.2 LABEL INFORMATIVENESS

**GNMDS Results:** We first repeat our GNMDS analyses from the theory and simulation sections on all the CIFAR-10 label variants for 200 high-entropy images (see Supplement). We use GNMDS to get triplet-respecting embeddings for each label type and then compute several metrics. As before, we compute Spearman correlations ( $\rho$ ) between the CIFAR-10 GNMDS and elicited similarity judgments. Our previous analyses assumed a consistent signal-to-noise ratio, or error rate, across all the label types. However, with our set of CIFAR-10 label variants coming from different participant pools and elicitation pipelines, it is likely that error rates will vary between label types. We approximate error rates of each label type by counting the proportion of triplet queries derived from the GNMDS embedding whose binary responses do not match the responses from the corresponding triplets computed from the human similarity judgments (i.e. the bit flip rate). Additionally, we compute

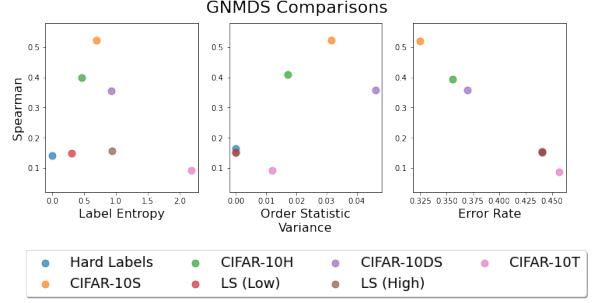


Figure 4: Correspondence between various metrics and Spearman rank correlation for each label variant.

label entropy and the variance of the first order statistic (i.e. variance of the probability mass assigned to the class with the highest assigned probability) for each label variant.

We visualize these results in Figure 4. We find that representation learning performance (measured by Spearman correlation) generally increases as softness (measured by entropy and variance) increases, but does not increase when smoothing hard labels. However, **we find there is a “sweet spot” for softness** after which performance begins to decrease. We also find the expected linear relationship between error rate and performance that our framework predicts. We hypothesize that the U-shaped relationship between softness and performance may partially be caused by increasing error rates, and partially by a resonance effect (see Supplement).

**Models:** We train diverse image classifiers on each of our supervision sets. These models have distinct architectural features and reflect seminal developments in the progression of natural-image classification (see Supplement).

**Cross-Label Performance:** We first assess how training classifiers on one set of soft labels impacts their validation performance when testing on other label types. Our primary measure of performance is crossentropy between the models’ predictive distributions and soft labels. Consistent with the GNMDS experiments, we observe a U-shaped relationship between label entropy and model performance for nearly all soft-label types (Figure 5, top row). The one exception is when testing on CIFAR-10DS labels, where training on higher levels of softness is preferred. These results suggest that, for image classification, *sparse soft labels*—of the kind collected in Collins et al. [2022] or formed via averaging [Peterson et al., 2019]—best capture the representational information expressed across different soft label sets. We also find that this relationship is preserved across different model architectures, with the Shake Shake model [Gastaldi, 2017] performing best across all label sets.

## 7.3 ZERO-SHOT GENERALIZATION

To further test how well image classifiers extract representational information from soft labels, we assess zero-shot generalization performance on increasingly out-of-distribution

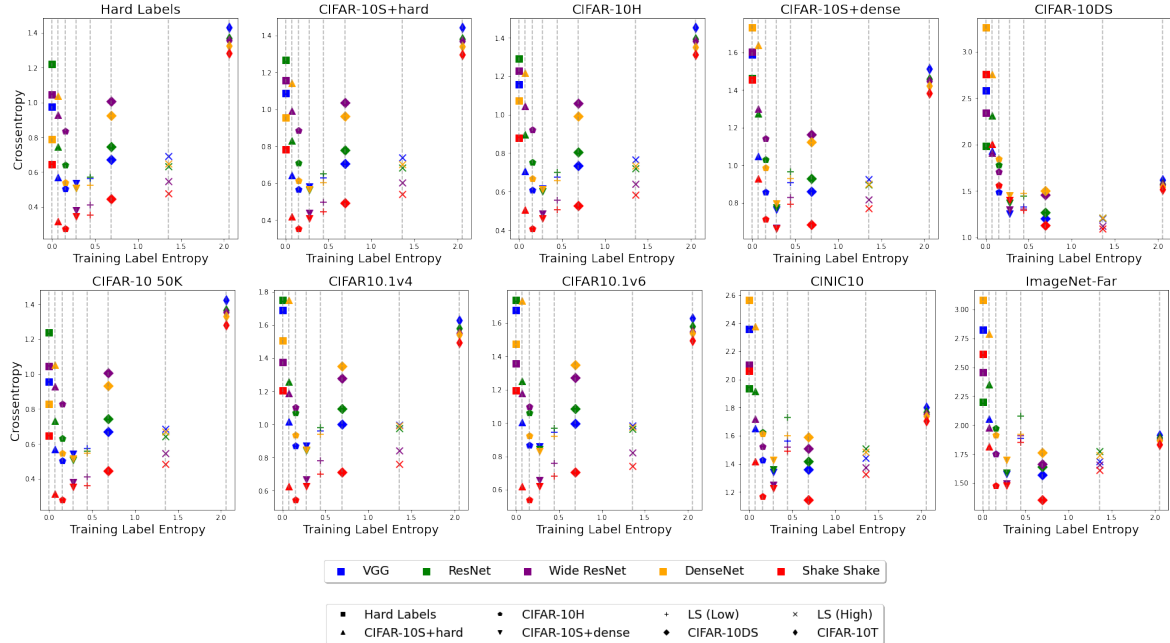


Figure 5: **Top:** Model performance on different label types at test time. **Bottom:** Generalization performance under increasing distributional shift. Each point represents the average score for a single model architecture (specified by color), trained on a particular label type (indicated via shape). Vertical lines represent points for a given label type.

image sets (Figure 5, bottom row; see Supplement). We find that for near-distribution datasets (CIFAR-10 50K [Krizhevsky et al., 2009]; CIFAR10.1v6, v4 [Recht et al., 2018]), classifier performance follows the U-shaped relationship described above. However, for far-distribution datasets (CINIC [Darlow et al., 2018], ImageNet-Far [Peterson et al., 2019]) a different pattern emerges. As found in Peterson et al. [2019], **soft labels increasingly outperform hard labels as distribution shift increases**. The improved relative performance of the CIFAR-10DS-trained networks supports this – although these labels are the most noisy, they also contain the richest supervision signal. It may be that more expressive classifiers are needed to fully capitalize on this richness [Battleday et al., 2020, Singh et al., 2020].

## 7.4 LEARNING FROM SMALL DATA

We empirically investigate our theoretical observation that softness is beneficial in the small data regime. Table 1 presents model performance with 80 or 8 training examples per class. We find that soft labels outperform hard labels, and the same general pattern between softness and performance holds.

## 8 DISCUSSION

In this paper, we offer a principled set of theoretical and empirical findings aimed at helping researchers to determine which form of supervisory signal they ought to collect for

the task at hand. We have provided theoretical grounding for how hidden representations can be recovered through supervised classification and have related the quality of these recovered representations to training parameters such as number of labels, classes, and dimensions. We found that while hard labels and soft labels provide comparable amounts of information in the many-examples-but-few-classes regime, soft labels become increasingly preferable when the number of classes increases or the number of labels decreases. Our findings explain why, for example, pre-training a classifier on ImageNet1K (1,000 classes) or ImageNet21k (21,000 classes) using hard labels may lead to decent transfer learning performance [Huh et al., 2016, Ridnik et al., 2021] but pre-training with (a form of) soft labels may lead to even better transfer learning performance [Xie et al., 2020]. We support our theoretical contributions with empirical results on a suite of human-derived soft labels. We include a compilation of practical guidance around human

Table 1: Small data regime results (crossentropy).

Labels	80 l/c	8 l/c
CIFAR-10	1.80	2.20
CIFAR-10S+hard	1.68	2.15
CIFAR-10H	<b>1.67</b>	2.15
CIFAR-10S+dense	1.69	<b>2.12</b>
CIFAR-10LS (Low)	1.73	2.19
CIFAR-10DS	1.70	<b>2.12</b>
CIFAR-10LS (High)	1.71	2.13
CIFAR-10T	2.10	2.25



soft label elicitation in the Supplement. We also note that our framework provides a general way to quantify the relative amount of information contained in each label by decomposing it into triplet queries (i.e., like a packet that contains a number of bits). This framework can be used with any representation learning setting where the goal is to efficiently recover hidden representations from an oracle (i.e., a person or another model) including classical supervised learning (which we focus on in this paper), knowledge distillation (getting a small student model to learn from a large teacher model), and contrastive learning (i.e., either via pairwise or triplet losses).

We note that, in our analysis, we made no assumptions about the data distribution in stimulus space, nor the function  $f(x_i) = z_i$  that maps from stimulus space to hidden representations, but when training neural networks we often assume some level of stability or invariance (i.e., a small perturbation in pixel space does not lead to drastically different perception of the image). When satisfied, inductive biases like assumptions about stability or invariance allow learners to extract additional information from training examples, sometimes even in an unsupervised way when no labels are present. As a result, our analysis here can be considered as a sort of lower-bound on how much information about hidden representations a labeled training dataset can provide. We also examined each supervision signal in isolation, assuming that only labels of one type are collected. A promising future direction would be to analyze additional sources of information (inductive biases, other supervision signals, etc.) as well as the interactions between them; already, we see promising indications of mixing label types in the case of CIFAR-10S+hard and CIFAR-10S+dense.

Notwithstanding these limitations, our analysis of hard labels, soft labels, and sparse labels that interpolate between them, already enables researchers to develop cost-benefit tradeoff curves in order to optimize the cost of labeling their datasets for supervised learning—and support the development of data-efficient, generalizable ML systems.

## Acknowledgements

This work was made possible by support from the NOMIS Foundation and the Office of Naval Research (N00014-18-1-2873) to TLG and an NSERC fellowship (567554-2022) to IS. KMC gratefully acknowledges support from the Marshall Commission and the Cambridge Trust. UB acknowledges support from DeepMind and the Leverhulme Trust via the Leverhulme Centre for the Future of Intelligence (CFI), and from the Mozilla Foundation. AW acknowledges support from a Turing AI Fellowship under grant EP/V025279/1, The Alan Turing Institute, and the Leverhulme Trust via CFI.

## References

- Sameer Agarwal, Josh Wills, Lawrence Cayton, Gert Lanckriet, David Kriegman, and Serge Belongie. Generalized non-metric multidimensional scaling. In *Proceedings of the Eleventh International Conference on Artificial Intelligence and Statistics*, pages 11–18, 2007.
- Ruairidh M Battleday, Joshua C Peterson, and Thomas L Griffiths. Capturing human categorization of natural images by combining deep networks and cognitive models. *Nature communications*, 11(1):5418, 2020.
- John Bridle. Training stochastic model recognition algorithms as networks can lead to maximum mutual information estimation of parameters. *Advances in neural information processing systems*, 2, 1989.
- Ting Chen, Simon Kornblith, Mohammad Norouzi, and Geoffrey Hinton. A simple framework for contrastive learning of visual representations. In *International conference on machine learning*, pages 1597–1607, 2020.
- Katherine M Collins, Umang Bhatt, and Adrian Weller. Eliciting and learning with soft labels from every annotator. In *Proceedings of the AAAI Conference on Human Computation and Crowdsourcing*, volume 10, pages 40–52, 2022.
- Luke Nicholas Darlow, Elliot J. Crowley, Antreas Antoniou, and Amos J. Storkey. CINIC-10 is not imagenet or CIFAR-10. *arXiv preprint arXiv:1810.03505*, 2018.
- Mark A. Davenport. Lost without a compass: Nonmetric triangulation and landmark multidimensional scaling. In *2013 5th IEEE International Workshop on Computational Advances in Multi-Sensor Adaptive Processing (CAMSAP)*, pages 13–16, 2013.
- Jacob Devlin, Ming-Wei Chang, Kenton Lee, and Kristina Toutanova. BERT: Pre-training of deep bidirectional transformers for language understanding. *arXiv preprint arXiv:1810.04805*, 2018.
- Li Fei-Fei, R. Fergus, and P. Perona. One-shot learning of object categories. *IEEE Transactions on Pattern Analysis and Machine Intelligence*, 28(4):594–611, 2006.
- Xavier Gastaldi. Shake-shake regularization. *arXiv preprint arXiv:1705.07485*, 2017.
- Wenzhong Guo, Jianwen Wang, and Shiping Wang. Deep multimodal representation learning: A survey. *IEEE Access*, 7:63373–63394, 2019.
- Greg Hanneman and Alon Lavie. Automatic category label coarsening for syntax-based machine translation. In *Proceedings of Fifth Workshop on Syntax, Semantics and Structure in Statistical Translation*, pages 98–106, 2011.

- Peter Harrison, Raja Marjieh, Federico Adolffi, Pol van Rijn, Manuel Anglada-Tort, Ofer Tchernichovski, Pauline Larrouy-Maestri, and Nori Jacoby. Gibbs sampling with people. *Advances in neural information processing systems*, 33:10659–10671, 2020.
- Kaiming He, Xiangyu Zhang, Shaoqing Ren, and Jian Sun. Deep residual learning for image recognition. In *Proceedings of the IEEE conference on computer vision and pattern recognition*, pages 770–778, 2016.
- Martin N Hebart, Charles Y Zheng, Francisco Pereira, and Chris I Baker. Revealing the multidimensional mental representations of natural objects underlying human similarity judgements. *Nature human behaviour*, 4(11):1173–1185, 2020.
- Alexander Hermans, Lucas Beyer, and Bastian Leibe. In defense of the triplet loss for person re-identification. *arXiv preprint arXiv:1703.07737*, 2017.
- Elad Hoffer and Nir Ailon. Deep metric learning using triplet network. In *International workshop on similarity-based pattern recognition*, pages 84–92, 2015.
- Gao Huang, Zhuang Liu, Laurens Van Der Maaten, and Kilian Q Weinberger. Densely connected convolutional networks. In *Proceedings of the IEEE conference on computer vision and pattern recognition*, pages 4700–4708, 2017.
- Minyoung Huh, Pulkit Agrawal, and Alexei A Efros. What makes ImageNet good for transfer learning? *arXiv preprint arXiv:1608.08614*, 2016.
- Kevin G Jamieson and Robert D Nowak. Low-dimensional embedding using adaptively selected ordinal data. In *2011 49th Annual Allerton Conference on Communication, Control, and Computing (Allerton)*, pages 1077–1084. IEEE, 2011.
- Aditi Jha, Joshua C Peterson, and Thomas L Griffiths. Extracting low-dimensional psychological representations from convolutional neural networks. *Cognitive Science*, 47(1):e13226, 2023.
- Prannay Khosla, Piotr Teterwak, Chen Wang, Aaron Sarna, Yonglong Tian, Phillip Isola, Aaron Maschinot, Ce Liu, and Dilip Krishnan. Supervised contrastive learning. *Advances in Neural Information Processing Systems*, 33:18661–18673, 2020.
- Diederik P Kingma and Max Welling. Auto-encoding variational Bayes. *arXiv preprint arXiv:1312.6114*, 2013.
- Alex Krizhevsky, Geoffrey Hinton, et al. Learning multiple layers of features from tiny images. 2009.
- Alex Krizhevsky, Ilya Sutskever, and Geoffrey E Hinton. Imagenet classification with deep convolutional neural networks. *Communications of the ACM*, 60(6):84–90, 2017.
- Maksim Lapin, Matthias Hein, and Bernt Schiele. Analysis and optimization of loss functions for multiclass, top-k, and multilabel classification. *IEEE transactions on pattern analysis and machine intelligence*, 40(7):1533–1554, 2017.
- Weiyang Liu, Zhen Liu, Hanchen Wang, Liam Paull, Bernhard Schölkopf, and Adrian Weller. Iterative teaching by label synthesis. In *NeurIPS*, 2021.
- Maya Malaviya, Ilia Sucholutsky, Kerem Oktar, and Thomas L Griffiths. Can humans do less-than-one-shot learning?, Jun 2022. URL <https://escholarship.org/uc/item/486752zx>.
- Raja Marjieh, Pol van Rijn, Ilia Sucholutsky, Theodore R Sumers, Harin Lee, Thomas L Griffiths, and Nori Jacoby. Words are all you need? capturing human sensory similarity with textual descriptors. *arXiv preprint arXiv:2206.04105*, 2022.
- Andre Martins and Ramon Astudillo. From softmax to sparsemax: A sparse model of attention and multi-label classification. In *International conference on machine learning*, pages 1614–1623, 2016.
- Rafael Müller, Simon Kornblith, and Geoffrey E Hinton. When does label smoothing help? *Advances in neural information processing systems*, 32, 2019.
- Joshua C Peterson, Joshua T Abbott, and Thomas L Griffiths. Evaluating (and improving) the correspondence between deep neural networks and human representations. *Cognitive science*, 42(8):2648–2669, 2018.
- Joshua C Peterson, Ruairidh M Battleday, Thomas L Griffiths, and Olga Russakovsky. Human uncertainty makes classification more robust. In *Proceedings of the IEEE/CVF International Conference on Computer Vision*, pages 9617–9626, 2019.
- Benjamin Recht, Rebecca Roelofs, Ludwig Schmidt, and Vaishal Shankar. Do cifar-10 classifiers generalize to cifar-10? *arXiv preprint arXiv:1806.00451*, 2018.
- Tal Ridnik, Emanuel Ben-Baruch, Asaf Noy, and Lihi Zelnik-Manor. Imagenet-21k pretraining for the masses. *arXiv preprint arXiv:2104.10972*, 2021.
- Brett D Roads and Bradley C Love. Enriching ImageNet with human similarity judgments and psychological embeddings. In *Proceedings of the IEEE/CVF conference on computer vision and pattern recognition*, pages 3547–3557, 2021.

- Sambu Seo and Klaus Obermayer. Soft learning vector quantization. *Neural computation*, 15(7):1589–1604, 2003.
- Roger N Shepard. Multidimensional scaling, tree-fitting, and clustering. *Science*, 210(4468):390–398, 1980.
- Karen Simonyan and Andrew Zisserman. Very deep convolutional networks for large-scale image recognition. *arXiv preprint arXiv:1409.1556*, 2014.
- Pulkit Singh, Joshua C Peterson, Ruairidh M Battleday, and Thomas L Griffiths. End-to-end deep prototype and exemplar models for predicting human behavior. *arXiv preprint arXiv:2007.08723*, 2020.
- Iliia Sucholutskv, Nam-Hwui Kim, Ryan P Browne, and Matthias Schonlau. One line to rule them all: Generating LO-shot soft-label prototypes. In *2021 International Joint Conference on Neural Networks (IJCNN)*, pages 1–8. IEEE, 2021.
- Iliia Sucholutsky and Matthias Schonlau. ‘Less than one’-shot learning: Learning  $n$  classes from  $m < n$  samples. *Proceedings of the AAAI Conference on Artificial Intelligence*, 35(11):9739–9746, 2021a.
- Iliia Sucholutsky and Matthias Schonlau. Soft-label dataset distillation and text dataset distillation. In *2021 International Joint Conference on Neural Networks (IJCNN)*, pages 1–8. IEEE, 2021b.
- Naftali Tishby, Fernando C Pereira, and William Bialek. The information bottleneck method. *arXiv preprint physics/0004057*, 2000.
- Antonio Torralba, Rob Fergus, and William T Freeman. 80 million tiny images: A large data set for nonparametric object and scene recognition. *IEEE Transactions on Pattern Analysis and Machine Intelligence*, 30(11):1958–1970, 2008.
- V. N. Vapnik and A. Ya. Chervonenkis. On the uniform convergence of relative frequencies of events to their probabilities. *Theory of Probability & Its Applications*, 16(2):264–280, 1971. doi: 10.1137/1116025. URL <https://doi.org/10.1137/1116025>.
- Qizhe Xie, Minh-Thang Luong, Eduard Hovy, and Quoc V. Le. Self-training with noisy student improves imagenet classification. In *Proceedings of the IEEE/CVF Conference on Computer Vision and Pattern Recognition (CVPR)*, 2020.
- Sergey Zagoruyko and Nikos Komodakis. Wide residual networks. *arXiv preprint arXiv:1605.07146*, 2016.

## A PRACTICAL GUIDANCE ON HUMAN SOFT LABEL ELICITATION

Our framework provides users with a way to quantify the relative amount of information contained in each type of label so that they can optimize which labels to collect for their dataset. Specifically, the findings from our theory, simulations, and experimental results are that the relative informativeness of labels depends on three factors associated with the dataset (the number of labeled examples, the number of classes, and the latent dimensionality) and two factors associated with labels (error rate and sparsity). Out of these, most factors are not under the user’s control but the primary factor that users can control (in supervised learning settings) is label sparsity. Our guidance to users is thus the following:

- Use our framework to estimate the relative informativeness of the label types you are considering collecting. The key parameter to optimize is label sparsity so compute the informativeness of soft labels with different levels of sparsity.
- Pick out promising label types and run a small pilot study collecting each label type for a small set of objects. Compute error rates and per-label costs for each label type.
- Update the relative informativeness estimates based on error rates and calculate the cost-benefit tradeoff for each label type. Pick the type with the most favorable tradeoff.

For users who want a simpler procedure, we offer the following rule-of-thumb guidance: *Generally, softer labels are preferable in smaller data regimes (e.g. one-shot and less-than-one-shot learning) while harder labels are preferable in big data regimes (i.e. many-shot learning).*

## B LABEL OPTIMIZATION SIMULATIONS

See Figure 6.

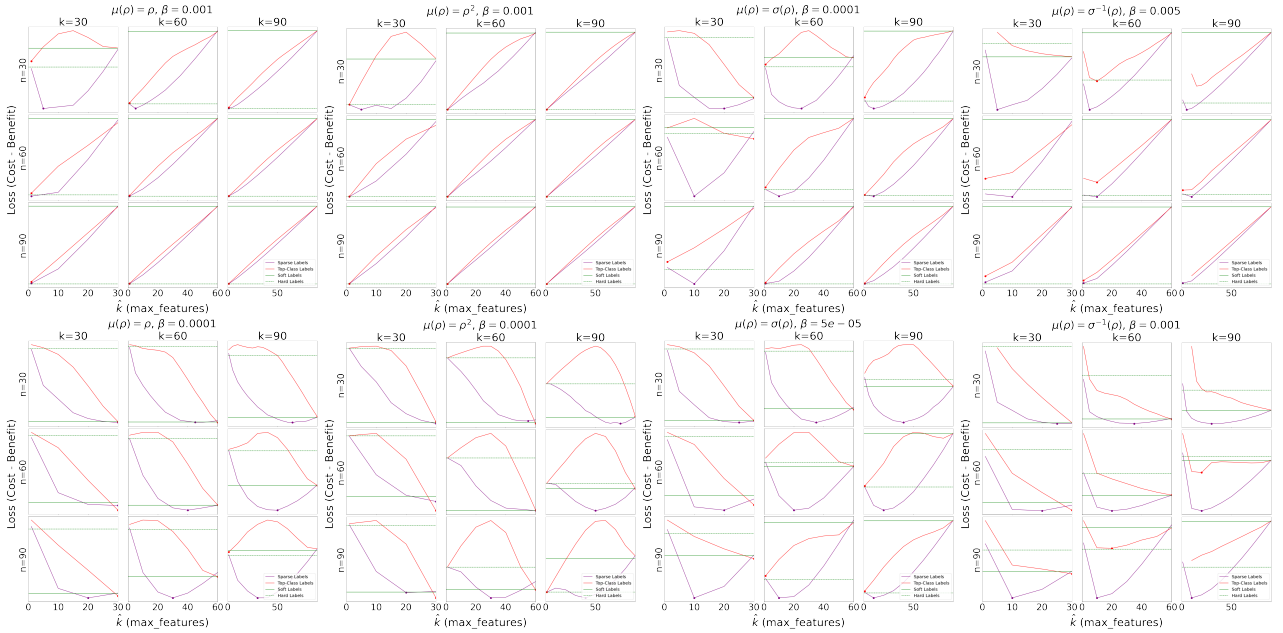


Figure 6: Loss curves for soft labels (solid green), sparse labels (purple), top-class labels (red), and hard labels (dashed green) based on subjective utility function ( $u(p)$ ), cost weighting parameter ( $\beta$ ), sparsity ( $\hat{k}$ ), number of points ( $n$ ), and number of classes ( $k$ ). Global minima for sparse labels and top-class labels are marked with a point.

## C ELICITED-HUMAN VS MODEL-PREDICTED ENTROPY

We investigate the hypothesis that the labels which confer the best downstream performance may strike a natural resonance with the models they are used as supervision signals for. In Figure 7, we compare the entropy of the training labels against the entropy of the trained models’ predicted distributions. In other words, we compare the probability distributions produced

by each model, to the probability distributions that the model was trained on. We find a remarkable alignment between the entropy of models’ predictions trained on the CIFAR-10S varieties. Future work could investigate the links between the inductive biases of models and the labels best suited for training specific architectures.

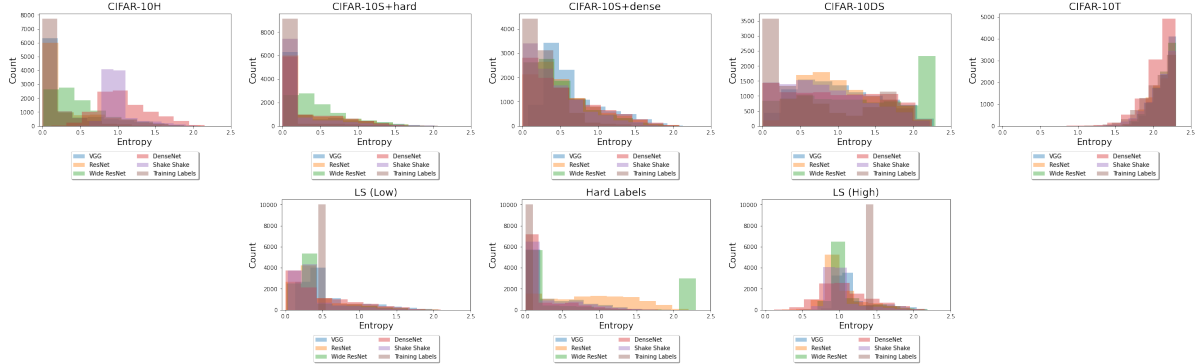


Figure 7: Comparing the entropy of the models’ predictions against the entropy of the labels used to train them. The training label type is listed as the title for the respective histogram.

## D ADDITIONAL DETAILS ON HUMAN SOFT LABELS

### D.1 COLLECTING CIFAR-10DS AND SIMILARITY JUDGMENTS

Soft labels for CIFAR-10DS, as well as similarity judgments, were collected on Amazon Mechanical Turk (AMT). The recruitment and experimental pipelines were automated using the PsyNet framework for online experiment design Harrison et al. [2020]. Prior to participation in the studies, participants provided informed consent in accordance with an Institutional Review Board (IRB), and were paid at a rate of \$12 per hour. In addition, participants were required to have successfully completed at least 2000 tasks on AMT.

To collect CIFAR-10DS, participants observed individual images and were given a set of sliders (10, one for each category) ranging from 0 to 1 and were asked to move the sliders in accordance with how well they thought each category matched a given image, with 0 being “not at all matching” and 1 being “completely matching”. We aimed for about 10 multi-ratings per image and each participant completed 50 such multi-ratings.

As for similarity judgments, participants were presented with pairs of unlabeled images and were required to rate their similarity on a 7-point Likert scale ranging from 0 (“completely dissimilar”) to 6 (“completely similar”). Here we aimed for 5 judgments per pair of images and each participant completed an average of 80 such judgments.

### D.2 IN-FILLING CIFAR-10S LABELS

The CIFAR-10S labels collected in Collins et al. [2022] included only 1,000 of the full 10,000 CIFAR-10 test set. Note, however, that these 1,000 examples were already enriched to be those that are naturally more confusing – so it can be considered a sensible sampling of what -10S labels *may* look like more generally. However, for adequate comparison against the other label types, we needed to choose a labeling method to label the remaining 9,000. We elected two variants: 1) using hard labels, or 2) simulating CIFAR-10S labels via sparsified version of CIFAR-10DS. The former represents a real-world cost efficient scenario; we could imagine a researcher only having the budget to annotate a subset of a dataset with soft labels. The second case is designed to mimic what the labels may have been like had we elicited CIFAR-10S over the full set. Taking only the scalar values for the top two highest sliders from CIFAR-10DS offered a nice entropy- and conceptual-match (entropy of 0.69 for CIFAR-10S to 0.75 for the adjusted -10DS labels). Future work could explore automated measures to extend label conversions (e.g., learning a mapping from CIFAR-10DS to simulated CIFAR-10S labels). We note that the CIFAR-10S labels used in this work are the T2 Clamp varieties, with a redistribution factor of 10% following Collins et al..

**CIFAR-10T** The CIFAR-10T labels are a novel set of labels we crowdsourced, comprising over 350,000 typicality ratings for each image under the ground truth category (about 35 judgements per image). 1759 unique participants were recruited on



Amazon Mechanical Turk, and presented with a sequence of 200 randomly sampled CIFAR-10 test set images, upsampled to 160x160 pixels (see Peterson et al. [2019], Battleday et al. [2020]). Participants were given the category of each image, and asked to rate how typical it was of the category on a sliding scale of “Not at all typical” to “Extremely typical”. We interpret an image’s typicality as the probability of the ground truth class, and spread the remaining probability mass over the 9 remaining labels—a smoothed version of a *sparse* soft label with  $K=1$ ).

### D.3 ADDITIONAL SIMILARITY JUDGMENT STUDIES

We extend the GNMDS analyses in the main text by examining the similarity structure of image representations extracted from the penultimate layer of each network. For each image and network, we derive an abstract vector representation by storing the unit activations of the last layer during classification. Then, for each image we compute the pairwise cosine similarity between the representations derived from our classifiers. We correlate these to the ground truth similarity ratings, and present the results in Figure 8. The images used for these analyses are discussed below, and displayed in Figures 11 and 12.

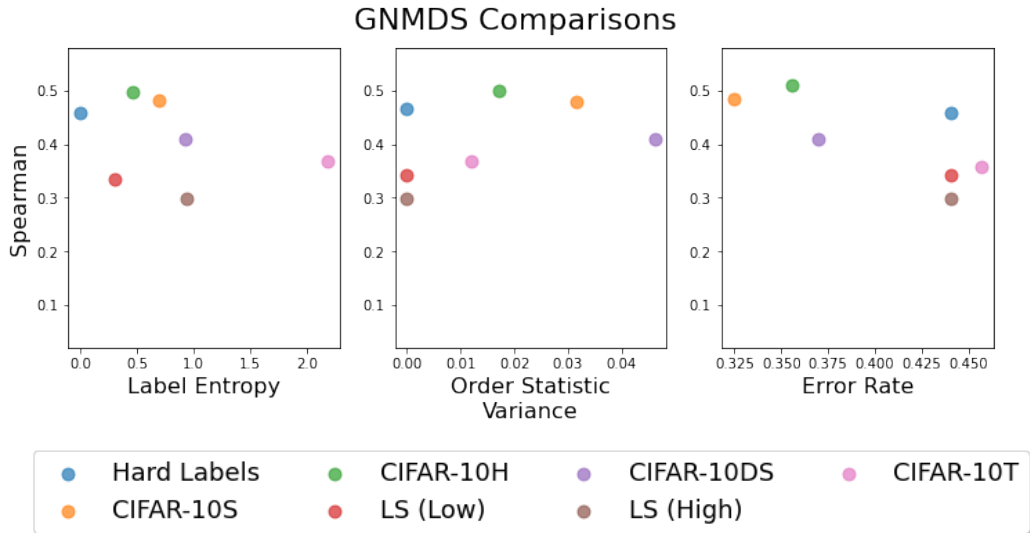


Figure 8: Correlation between ground-truth similarity judgments and the cosine similarity of image representations for different model architectures.

## E ADDITIONAL COMPUTATIONAL EXPERIMENT DETAILS AND OBSERVATIONS

### E.1 MODELS

We use ten fold cross-validation to partition the images of the CIFAR-10 test subset into train and validation sets for each set of soft labels. We train a number of models using stochastic gradient descent over a range of learning rates and seeds, and use the best performing seed for all subsequent analyses (Table 2). We use ten fold cross-validation to partition the images of the CIFAR-10 test subset into train and validation sets for each set of soft labels.

Table 2: Image Classifiers.

Model	Key Features	Parameters	Citation
VGG	very deep connections	14,728,266	Simonyan and Zisserman [2014]
ResNet	residual connections		He et al. [2016]
WRN	wide residual connections	36,479,194	Zagoruyko and Komodakis [2016]
DenseNet	dense connections	769,162	Huang et al. [2017]
Shake shake	shake shake regularization	11,709,514	Gastaldi [2017]

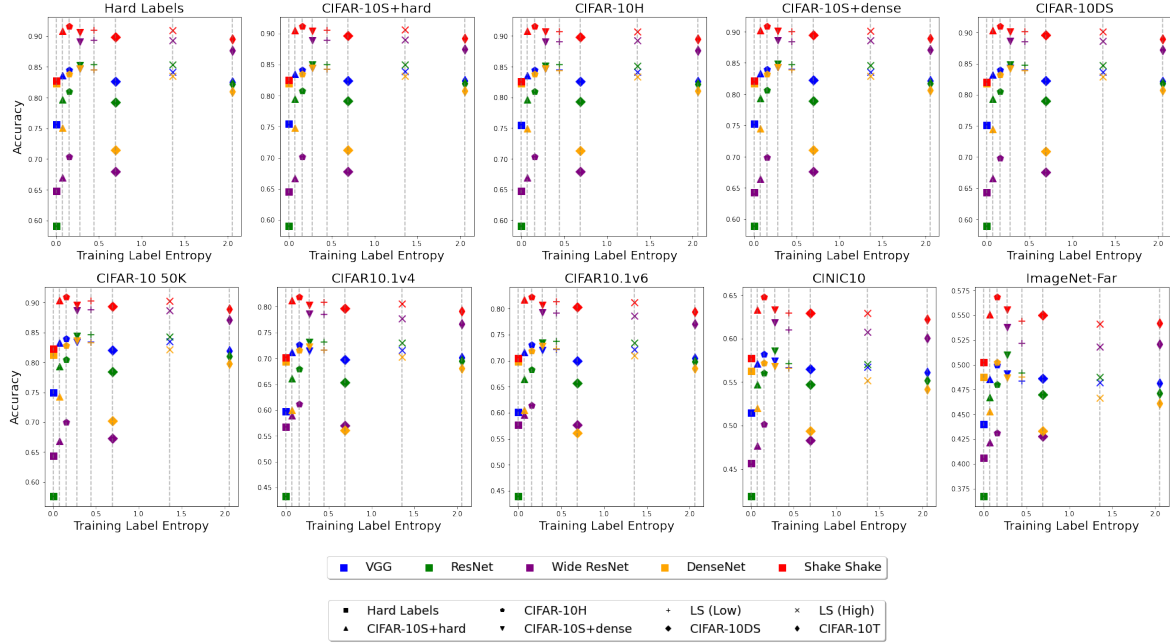


Figure 9: Cross-label (top) and generalization results (bottom), scored by top-1 accuracy against the respective labels.

## E.2 DATASETS

In order of increasing distributional shift, CIFAR-10 50K is the *training* subset of CIFAR10 (50,000 images; Krizhevsky et al. [2009]), CIFAR10.1v6, v4 are two near-sample datasets constructed from the same TinyImages classes Torralba et al. [2008] as CIFAR-10 (2,000 images each; Recht et al. [2018]), our subset of CINIC10 contains rescaled images from ImageNet using the CIFAR-10 classes (210,000 images; Darlow et al. [2018]), and ImageNet-Far contains a label-coarsened version of rescaled ImageNet images such that the CIFAR classes now contain a more diverse range of examples (for example, now “deer” contains “ibex” and “gazelle”; 63,895 images; Peterson et al. [2019], Darlow et al. [2018]).

## E.3 SOFTNESS, TASK ACCURACY, AND INFORMATION CONTENT

In the main text, we depicted the relationship between label softness and task performance using crossentropy (CE) as our principal metric. We focus on CE as it better captures the fidelity of the models’ predictive distributions. This is particularly important when we evaluate the model on held-out soft labels; CE offers more information about model performance than just top-1 accuracy. However, we include top-1 accuracy in Figure 9 for completeness.

We also depict performance in Figure 10 as function of the information content of the labels. Here, we use the Spearman rank correlation coefficient between the CIFAR-10 GNMDS and elicited similarity judgments as a proxy for information content. Note, here, CIFAR-10S+hard and CIFAR-10S+dense have the same score, as the similarity judgments are collected over the 1000 shared original CIFAR-10S examples.

## E.4 EFFECTIVE DIMENSIONALITY OF SOFT LABELS

Our theory and simulations address the number of features available for representation learning but did not discuss the nature of these features—i.e., whether they are essential or superfluous. Estimating the effective dimensionality of a dataset is tied to the nature of the computational task required. For classification, there is a range of methods for estimating this (e.g., [Vapnik and Chervonenkis, 1971, Jha et al., 2023]).

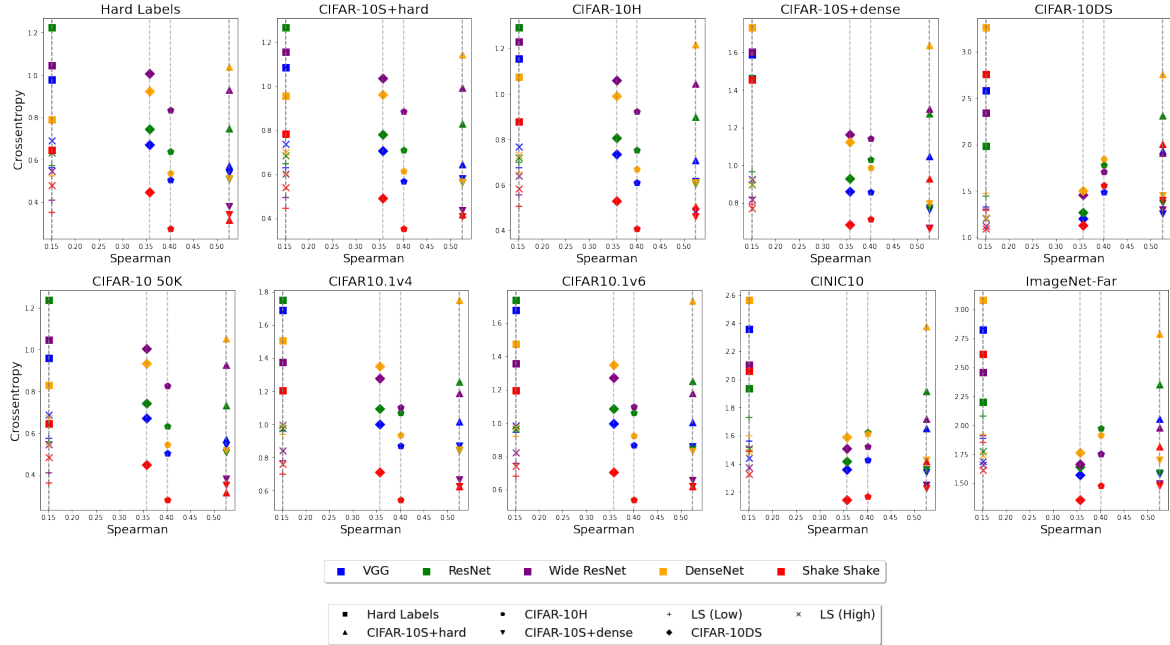


Figure 10: **Top:** Model performance on different label types at test time, as a function of information content of the labels. Information content is approximated by the Spearman rank correlation with similarity judgments. **Bottom:** Generalization performance under increasing distributional shift, as a function of training label information content.

Table 3: Crossentropy (lower is better) as a function of varying the classes we permit human uncertainty specification over.

Classes per Label	CIFAR10-50k	CIFAR10.1v4	CIFAR10.1v6	CINIC10	ImageNet-Far
$k = 2$	<b>0.46</b>	<b>0.77</b>	<b>0.76</b>	1.32	1.57
$k = 3$	0.48	<b>0.77</b>	<b>0.76</b>	1.30	1.51
$k = 4$	0.49	<b>0.77</b>	0.77	<b>1.26</b>	<b>1.47</b>
$k = 10$	0.76	1.09	1.08	1.40	1.60

## E.5 VARYING LABEL SOFTNESS

We further investigate how the amount of softness we elicit from humans when constructing our supervision signals impacts downstream performance: a selective ablation for increasing levels of sparsity. In our real-world soft label experiments, we in-fill missing CIFAR-10S labels by simulating if CIFAR-10DS labels had only provided uncertainty over  $\hat{k} = 2$  labels. As we have softness over all  $k = 10$ , we can simulate varying  $\hat{k}$ . We train additional models in-filling with  $\hat{k} = 3$  and 4, respectively. We find that the extra softness does not add substantial value over  $\hat{k} = 2$  when evaluating on near-domain generalization (i.e. CIFAR10-50k, .1v4, and .1v6), but does appear to have a positive effect when evaluating on further out-of-domain generalization (e.g., CINIC10 and ImageNet-Far).

## E.6 REPRESENTATIVE IMAGES AND MODEL PREDICTIONS

In Figures 11 and 12 we present the images used as the basis of the similarity experiments (see above for details on label and similarity judgment collection). These images were chosen *using our trained classification models* to include images that were likely to have high label entropy (Figure 11), and images where model predictions diverged (Figure 12). The models making the predictions had not been trained on these images (i.e., the predictions were based on the held-out cross-validation folds).

In Figures 13-22, we present four exemplars from each class, along with the soft labels and model predictions. We see that this analysis picks out genuinely ambiguous images, with borderline cases between two classes, many classes, noisy images, and categorically uncertain images. For each image, the top row are images in which models agree on high likely entropy (average prediction entropy). The bottom row is where models maximally disagree (average symmetric relative entropy).

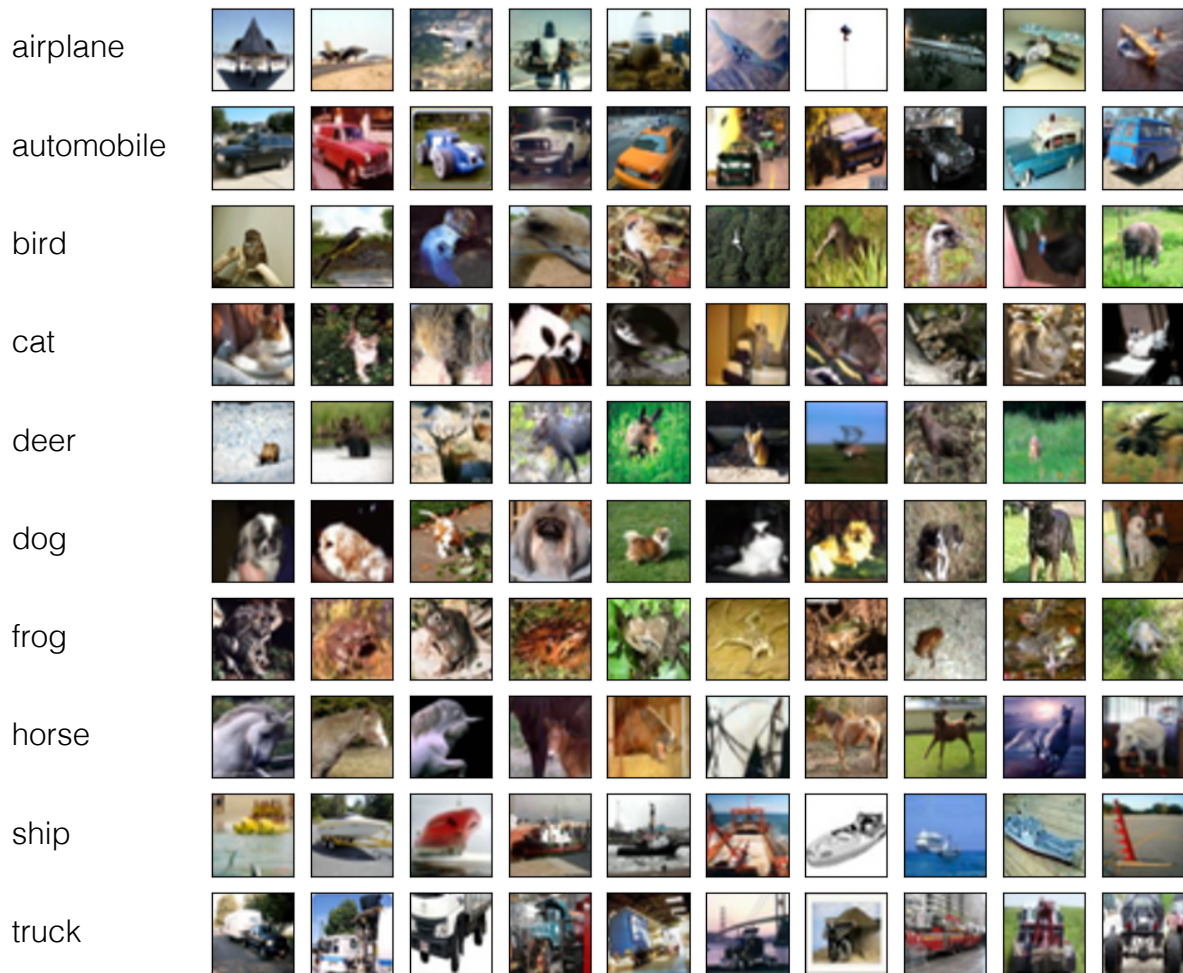


Figure 11: 100 images from the CIFAR-10 testing subset. These were chosen to include images that were likely to have high label entropy.

between pairwise comparisons of models).

## F ENLARGED MAIN RESULTS FIGURE

See Figure 23.

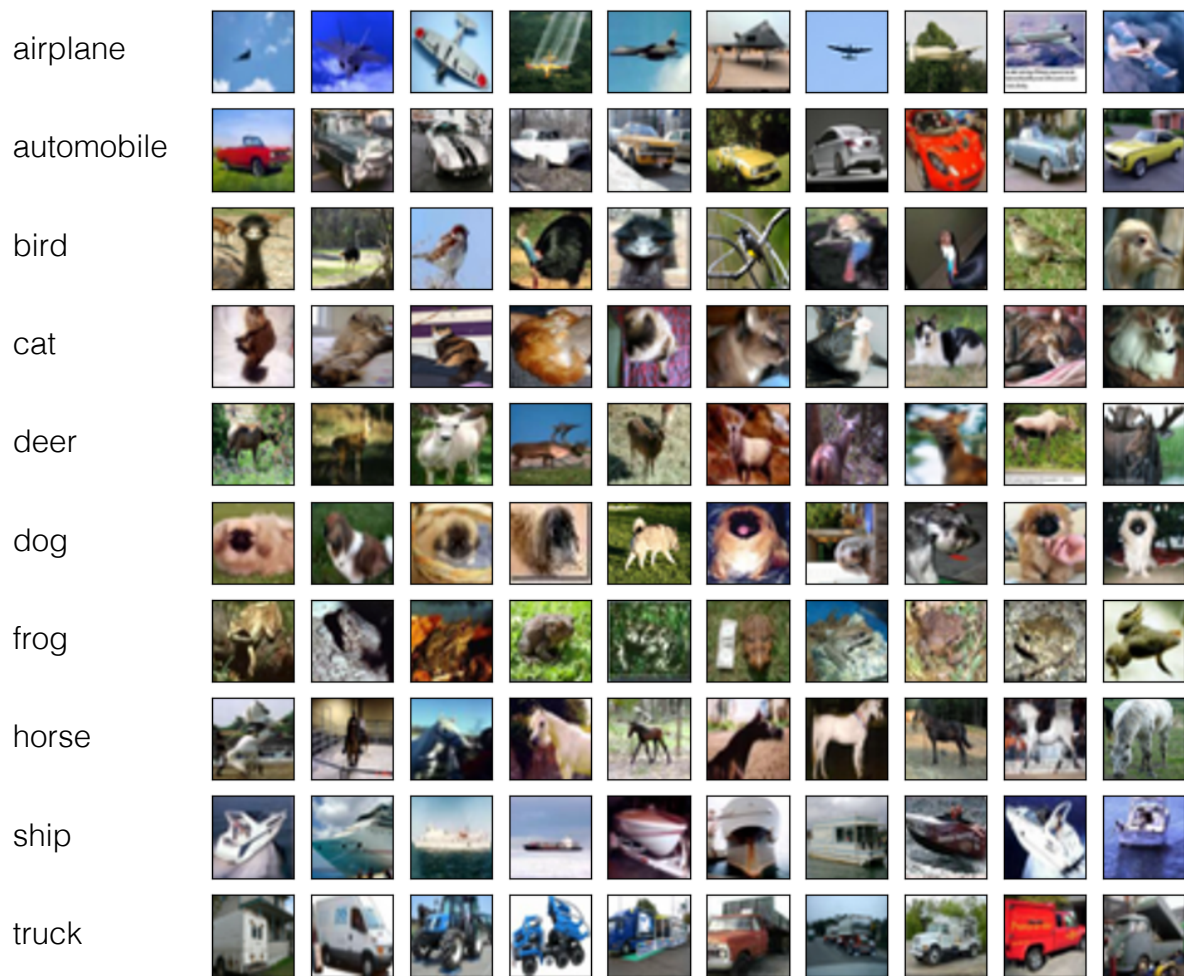


Figure 12: 100 images from the CIFAR-10 testing subset. These were chosen to include images that were likely to cause model disagreement.



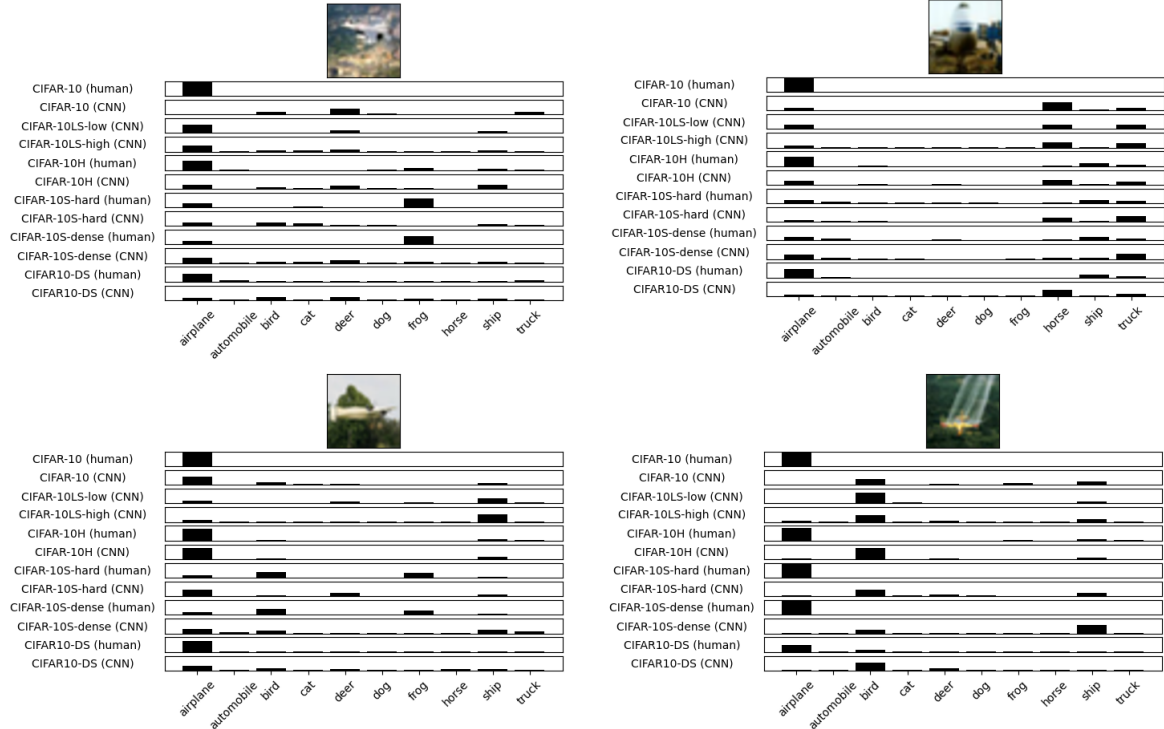


Figure 13: Representative ambiguous plane images. Top row: model agreement on high entropy image. Bottom row: maximal model disagreement.

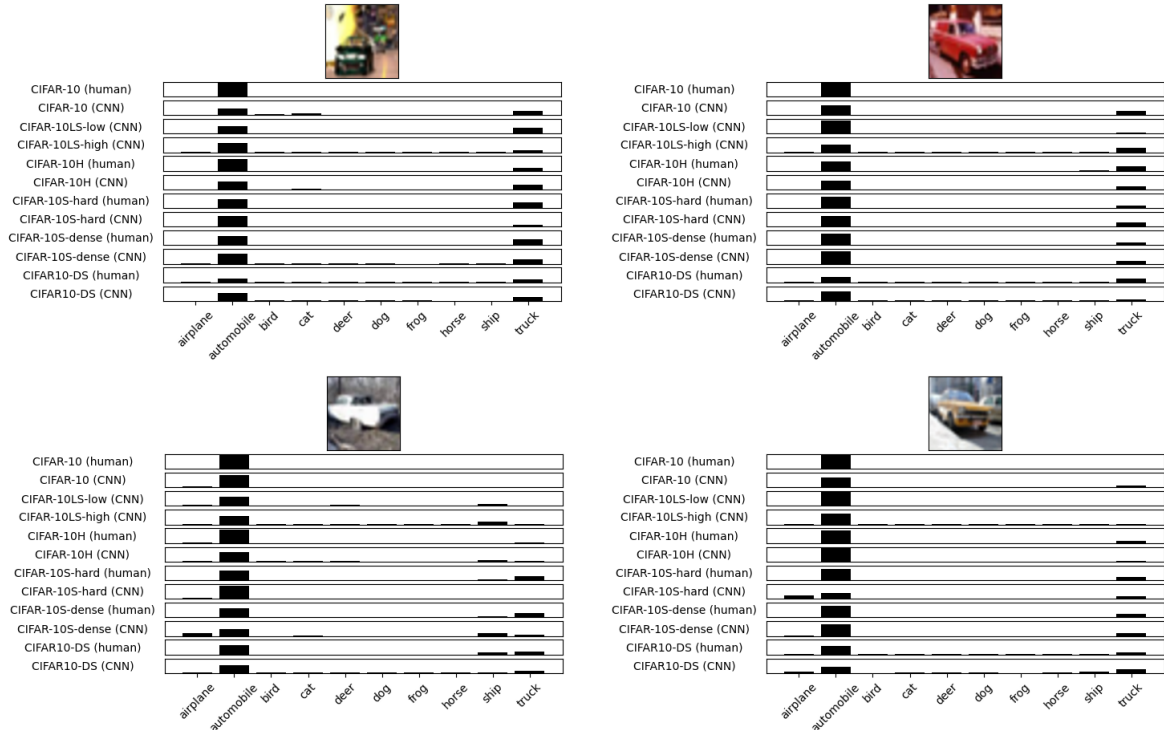


Figure 14: Representative ambiguous automobile images. Top row: model agreement on high entropy image. Bottom row: maximal model disagreement.

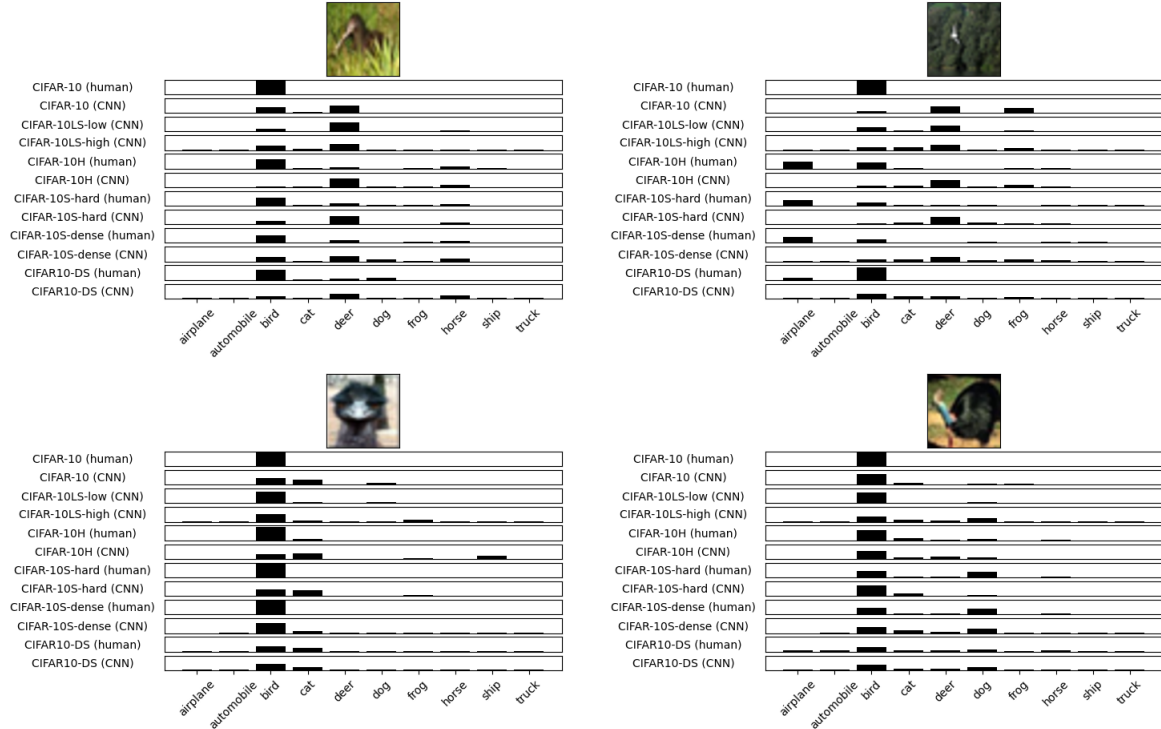


Figure 15: Representative ambiguous bird images. Top row: model agreement on high entropy image. Bottom row: maximal model disagreement.

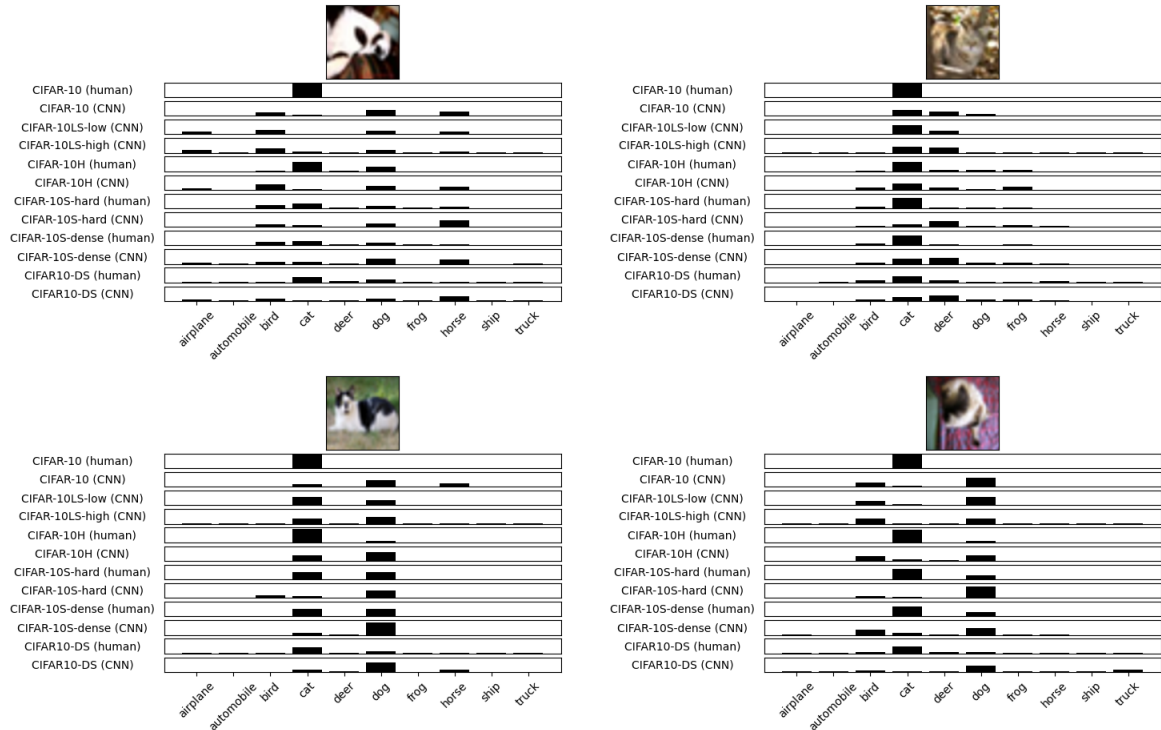


Figure 16: Representative ambiguous cat images. Top row: model agreement on high entropy image. Bottom row: maximal model disagreement.

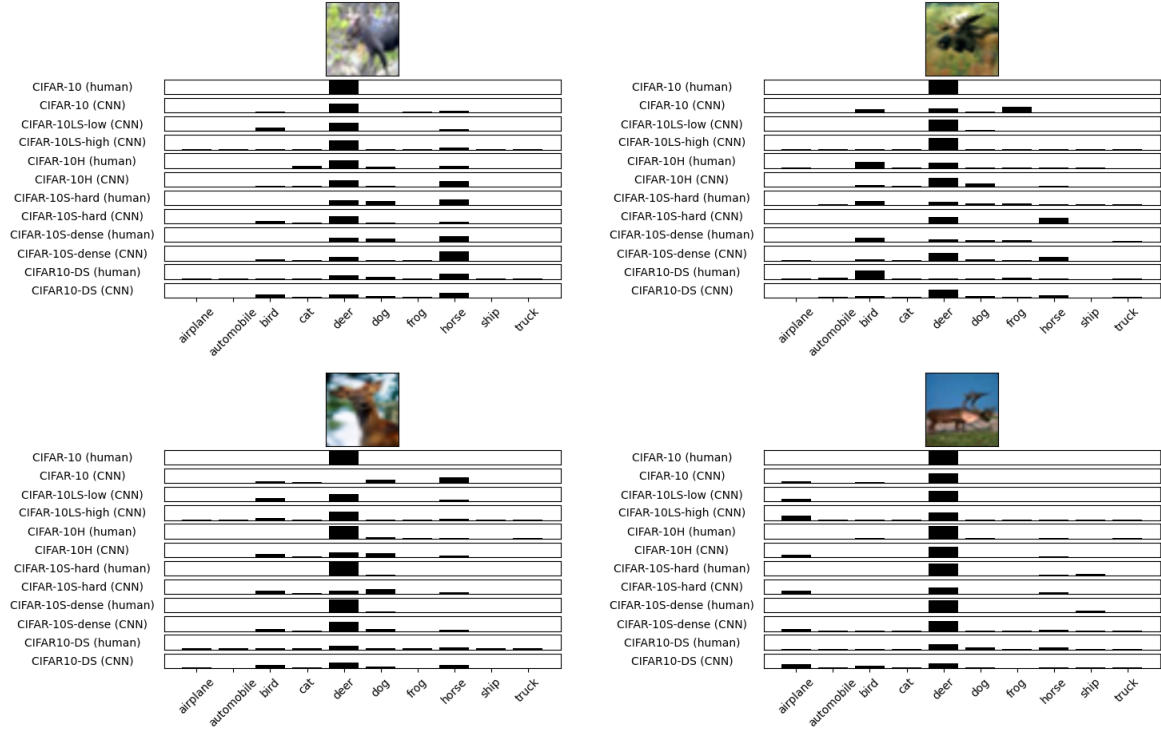


Figure 17: Representative ambiguous deer images. Top row: model agreement on high entropy image. Bottom row: maximal model disagreement.

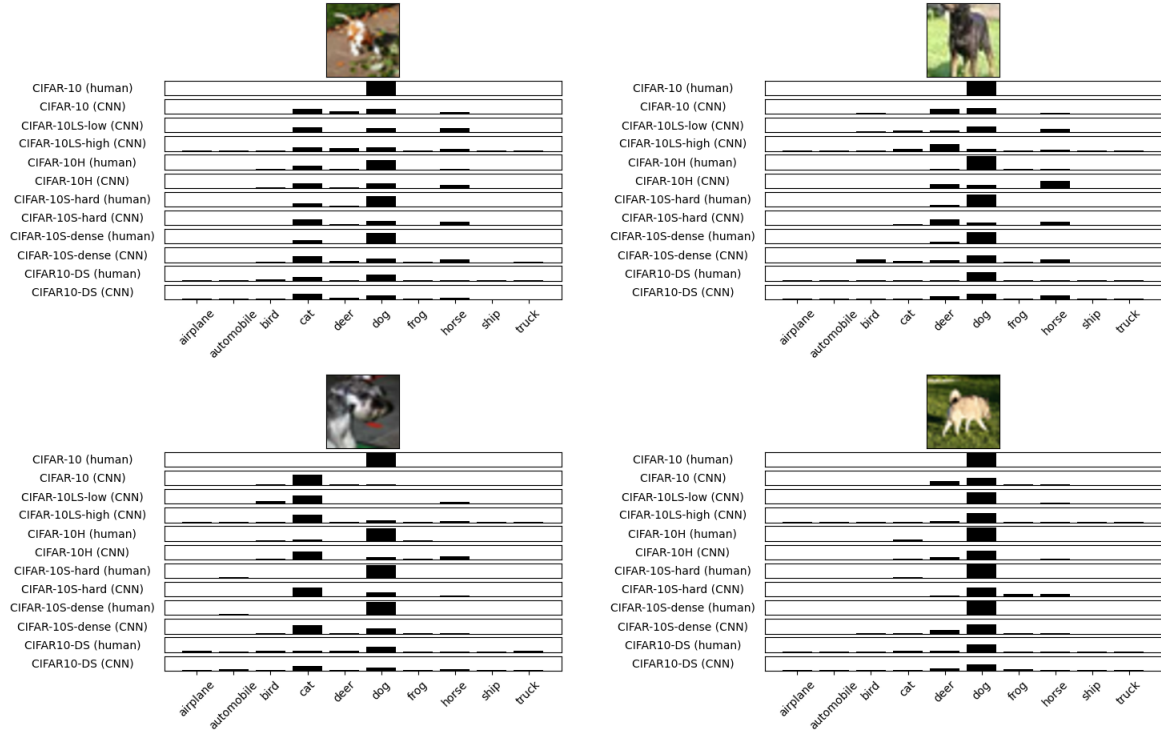


Figure 18: Representative ambiguous dog images. Top row: model agreement on high entropy image. Bottom row: maximal model disagreement.

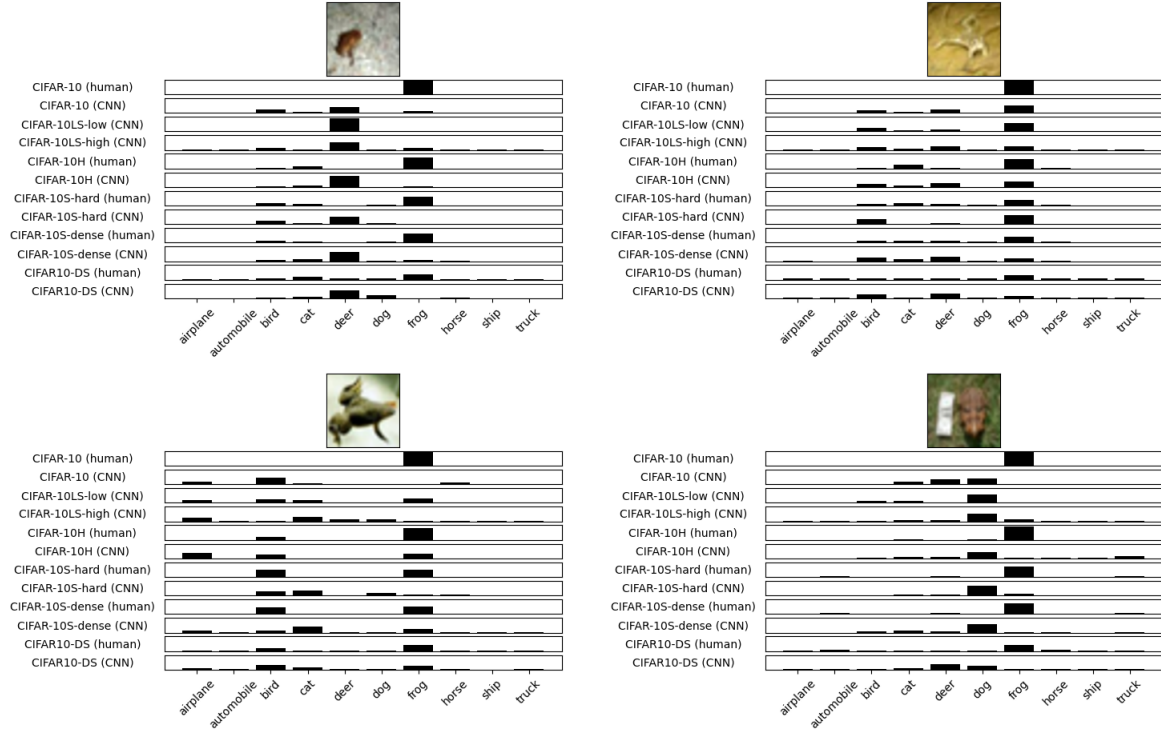


Figure 19: Representative ambiguous frog images. Top row: model agreement on high entropy image. Bottom row: maximal model disagreement.

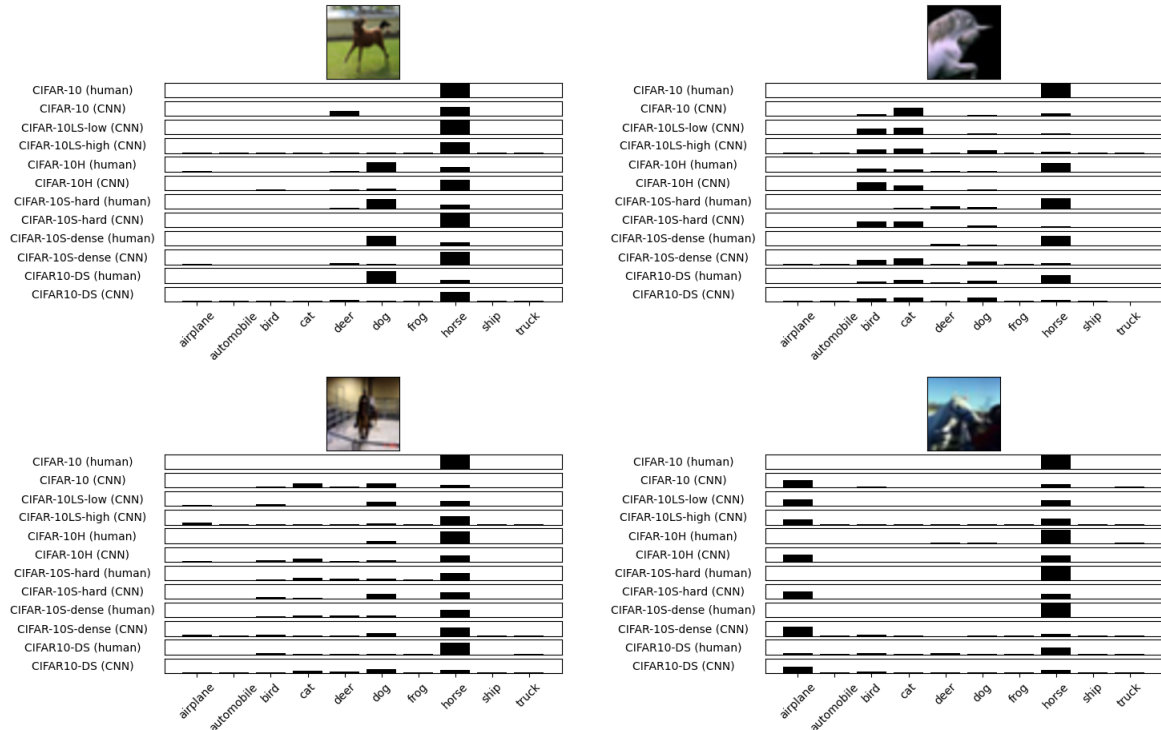


Figure 20: Representative ambiguous horse images. Top row: model agreement on high entropy image. Bottom row: maximal model disagreement.

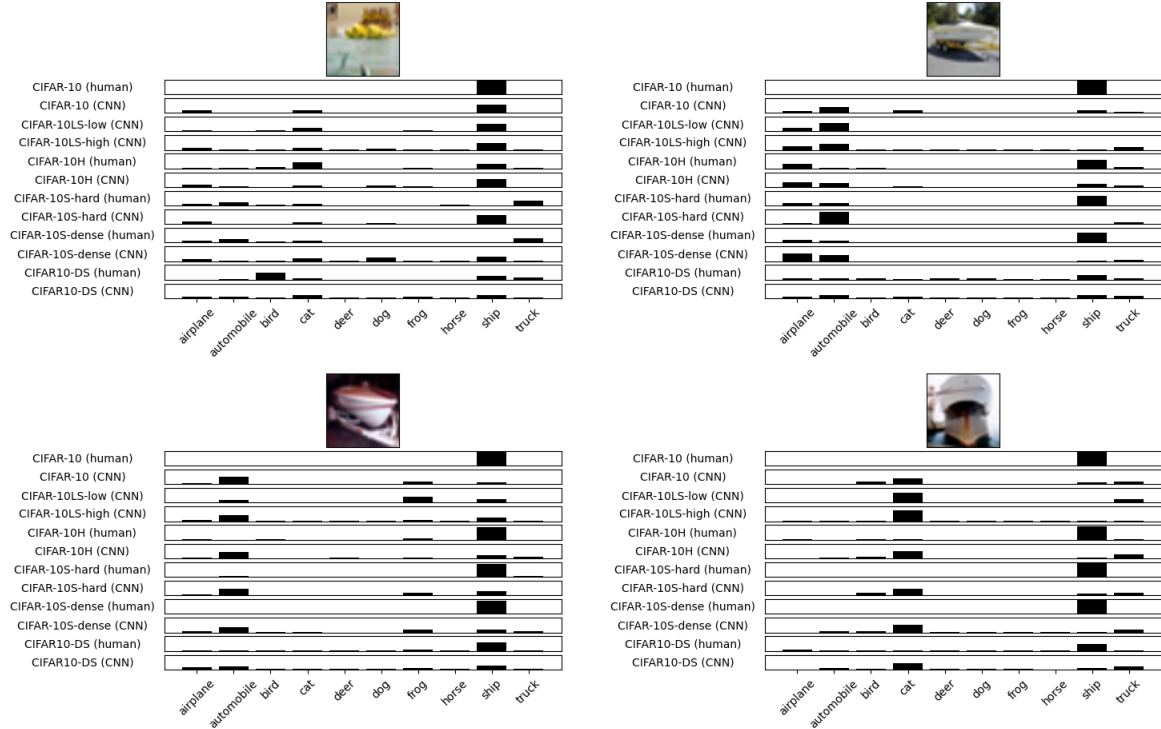


Figure 21: Representative ambiguous ship images. Top row: model agreement on high entropy image. Bottom row: maximal model disagreement.

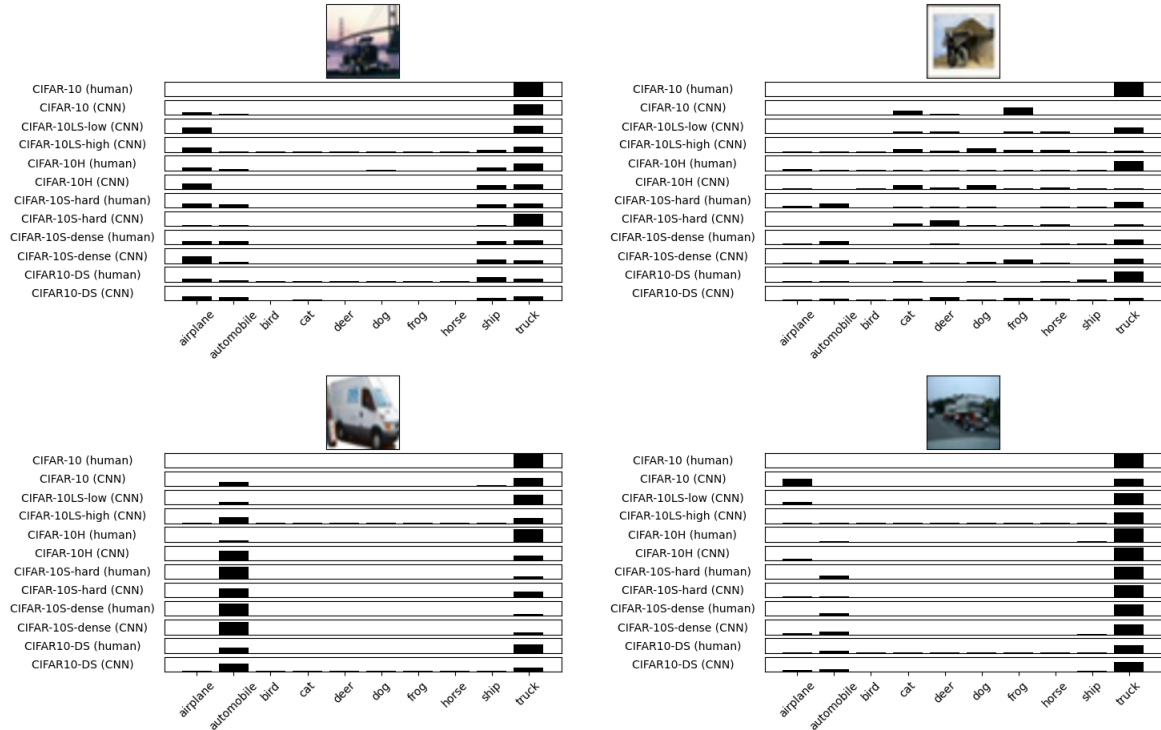


Figure 22: Representative ambiguous truck images. Top row: model agreement on high entropy image. Bottom row: maximal model disagreement.



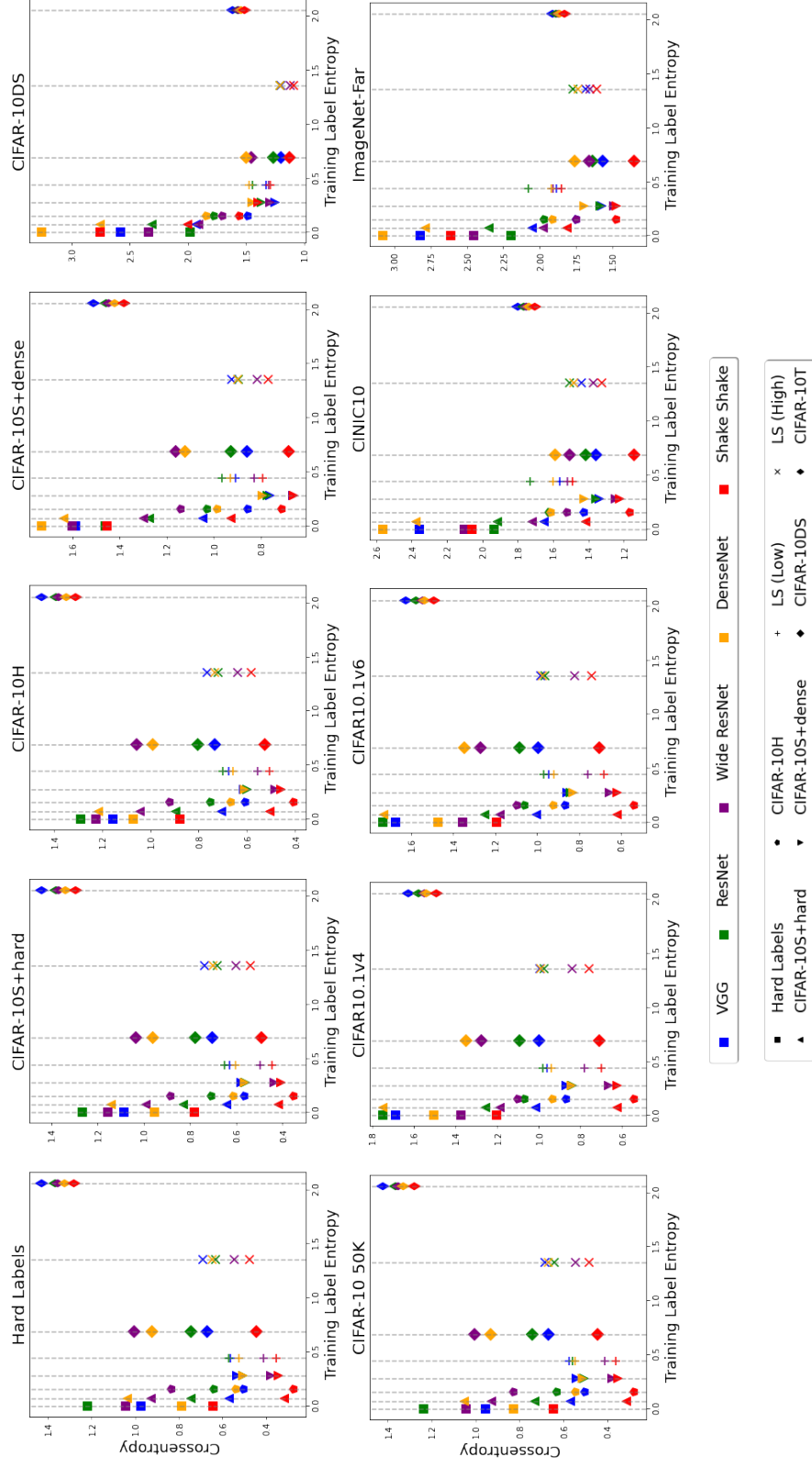


Figure 23: **Top:** Model performance on different label types at test time. **Bottom:** Generalization performance under increasing distributional shift. Each point represents the average score for a single model architecture (specified by color), trained on a particular label type (indicated via shape). Vertical lines represent points for a given label type.